RECALIBRATION OF THE VESTIBULAR SYSTEM

by

Tammy Che-Yan Law

A THESIS SUBMITTED IN PARTIAL FULFILLMENT OF THE REQUIREMENTS FOR THE DEGREE OF

MASTER OF SCIENCE

in

The Faculty of Graduate Studies

(Human Kinetics)

THE UNIVERSITY OF BRITISH COLUMBIA
(Vancouver)

July 2011

Abstract

The vestibular system conveys information regarding head motion to the central nervous system (CNS). Independently, this vestibular signal of head motion does not provide an absolute reference of head motion as the frequency coding of the afferent nerves is influenced by adaptation properties and nonlinearities. The optic flow signal of head rotation from the visual system however, is spatially encoded and can function as an absolute reference. The aim of this study was to determine if a visual signal of head rotation can recalibrate an altered vestibular signal of head motion during standing balance and to investigate the underlying mechanisms of this recalibration at the muscular level.

Eight healthy subjects were exposed to an electrical vestibular stimulus correlated to head movement (±0.125 mA/°/s) while standing on foam with eyes closed. This velocity-coupled vestibular stimulation (VcVS) was applied in a bipolar, bilateral orientation and depending on its polarity, resulted in the vestibular nerves coding for slower or faster head movements. Initially, this alteration of natural vestibular information destabilized subjects. During the conditioning phase, subjects opened their eyes and used visual information in combination with the new vestibular information to update their representation of self-orientation. Following this, subjects showed a significant decrease (~35%) in body sway while still receiving VcVS.

The mechanisms underlying vestibular recalibration were examined by observing how visuo-vestibular recalibration affected the vestibular-evoked muscular responses. Muscle activity was recorded in five subjects using surface electromyography (EMG) bilaterally on the medial gastrocnemius and tensor fascia latae muscles. Stochastic vestibular stimulation (SVS) in combination with VcVS was delivered to evoke biphasic muscular responses. Prior to the conditioning period, the peak amplitude of the response was significantly attenuated and then returned to control levels following conditioning.

Overall, these observations indicate that the vestibular system can be recalibrated by a visual signal of head rotation. This process is associated with an initial decrease in vestibular-evoked muscular responses which return to control levels once recalibration occurs. These results suggest that the CNS can modulate vestibular processes by down regulation or selective gating of vestibular signals in order to achieve vestibular recalibration.

Preface

The study protocol was approved by the Clinical Research Ethics Board of the University of British Columbia; Ethics Certificate number H10-02460.

Table of Contents

List of Tables

List of Figures

Acknowledgements

My thesis would not have been possible if it weren't for a handful of amazing people. To them, I'd like to express my tremendous gratitude. First and foremost, I'd like to thank my supervisor, Dr. Jean-Sébastien Blouin for challenging me every day and guiding me to accomplish above and beyond what I thought was possible. Thank you for teaching me how to learn. A very special thank you goes to Dr. Martin Héroux, for being both a mentor and a friend since day one. My grad school experience would not have been nearly as enjoyable (or gaseous) without you. I'd also like to thank Dr. Romeo Chua for being a part of my committee and providing me with many helpful ideas and comments along the way. To my other lab mates, Chris Dakin, Billy Luu, Daniel Mang and Harrison Brown, thank you for all the laughs, lessons, advice and memories…and for treating me like one of the guys (maybe a little too much sometimes). I couldn't have asked for a better, more fantastic group of colleagues to work with. To all my subjects, thank you for volunteering your time to make my project possible.

On a more personal note, I'd like to thank my friends for always believing in me and for listening to all my rants and ravings. I'd like to thank Codie for being a constant source of comfort on all the weekends and late nights spent at the lab. Last but not least, I'd like to dedicate this thesis to Mom, Dad, Alvin and the rest of my family: thank you for your unwavering love and never ending support.

"How do I love you, thesis? Let me count the ways…
I think about you night and day
I see you in my dreams
I sing your praises far and wide
I write odes to you no one will ever read
I weep at your absence
I count the ~~days~~ years until you're mine"

- Jorge Cham, PhD Comics

Introduction

As a contributor to standing balance in humans, the vestibular system[1] provides the central nervous system (CNS) with information regarding linear and angular head motion. Distinct from other senses, the vestibular system does not produce an overt conscious sensation. Rather, vestibular information sent to the CNS becomes integrated with other sensory information and thus contributes to a wide range of functions (Angelaki & Cullen, 2008). Recently, vestibular sensory feedback has been shown to play a role in the representation of head motion in space. In a study by Day and Reynolds (2005), subjects were exposed to electrical stimulation of the vestibular system coupled to angular head velocity. This velocity-coupled signal was compatible with natural vestibular stimulation but with a higher or lower frequency gain. Thus, for a given head movement, the afferent firing frequency coded for a signal of faster or slower head rotations. In the absence of visual information, subjects adjusted their movements accordingly to the altered vestibular input. These results demonstrate that the altered vestibular information was interpreted as arising from real head movements and utilized this information when generating motor commands. Similarly, St George and Fitzpatrick (2010) showed that subjects interpret electrical vestibular stimulation as real rotations by making compensatory responses during rotational stepping tasks. They have proposed that in general, when a sensation of self-motion arises from an externally applied signal, the feedback of other sensory systems are recalibrated by the process of sensory fusion[2] to maintain a single representation of self-motion with respect to the external world.

---

[1] Refer to *Appendix A - Anatomy of the Vestibular System* and *Physiology and Biomechanics of the Vestibular System* for more information

[2] Refer to *Appendix A - Theoretical frameworks* for more information

The signal of head rotation from the vestibular system is frequency encoded by the semicircular canals and otolith organs and transmitted in the vestibular nerves (Baloh & Honrubia, 2001). As the relationship between afferent discharge rate and head movement is not constant due to adaptation properties and small nonlinearities (Fernandez & Goldberg, 1971), this encoding cannot provide the CNS with a fixed reference of head rotation. Conversely, the visual signal on the retina is spatially encoded (Bear *et al.*, 2007), allowing the optic flow signal associated with head rotation to provide a more stable reference. Here, our objectives are to first, determine whether the gain of the vestibular system can be recalibrated by a visual signal of head rotation, and second, to investigate the physiological mechanisms of this recalibration at the muscular level.

In Experiment 1, we measured the body sway of subjects who were exposed to electrical vestibular stimulation coupled to head velocity (velocity-coupled vestibular stimulation, VcVS). Electrical stimulation of the vestibular nerves, a technique commonly known as galvanic vestibular stimulation (GVS)[3] (for a review, see Fitzpatrick & Day, 2004) evokes an artificial signal of head roll about the GVS-vector axis[4] (Day & Fitzpatrick, 2005). Since the effects of real rotations and electrical stimulation on the vestibular nerves are thought to summate linearly (Lowenstein, 1955), coupling head motion to current intensity enabled us to increase or decrease the vestibular afferent response, imitating a firing frequency corresponding to a faster (additive signal) or slower (subtractive signal) head movement. We hypothesized that the amount of body sway caused by VcVS would decrease after a period of visual conditioning and that when the stimulus was turned off, body sway would increase indicating after-effects of the recalibration.

---

[3] Refer to *Appendix A - Galvanic Vestibular Stimulation* for more information
[4] Refer to *Appendix A - GVS-Vector Sum Model* for more information

To elucidate possible underlying physiological processes associated with vestibular recalibration, we examined vestibular-evoked muscular responses[5] bilaterally in the medial gastrocnemius and tensor fascia latae muscles before and after conditioning in Experiment 2. Responses were evoked by combining low amplitude stochastic vestibular stimulation (SVS) to VcVS. We hypothesized that when a vestibular signal of faster head motion is recalibrated, the corresponding muscular responses would be decreased to represent a down regulation of the original vestibular signal. Similarly, when a vestibular signal of slower head motion is recalibrated, the corresponding muscular responses would be increased to represent an up regulation of the original vestibular signal.

---

[5] Refer to *Appendix A - GVS-evoked Muscle Responses* for more information

Methodology

Subjects

Eight healthy volunteers (27.3 ± 4.7 years, 6M 2F) participated in Experiment 1 and of those eight, five (28.4 ± 5.8 years, 3M 2F) participated in Experiment 2. All subjects had no known history of neurological disease or injury. All subjects were able to balance for at least 60 s standing with feet together on a foam pad with eyes closed. Written consent was obtained from every subject after the general procedures of the study were explained. The study protocol was approved by the Clinical Research Ethics Board of the University of British Columbia and all procedures were conducted in accordance to the *Declaration of Helsinki*.

Vestibular Stimuli

Electrical vestibular stimulation was delivered through carbon-rubber electrodes (9 cm^2) coated with conductive gel (Spectra 360, Parker Laboratories, Fairfield, USA) and securely fixed over the mastoid processes bilaterally. The main stimulus in this study was coupled to head angular velocity and was delivered to the subjects via a constant current stimulus isolator (Stimsol, BIOPAC Systems Inc, Goleta, CA, USA) with limits set to ± 9.5 mA. Figure 1 shows the experimental set-up and generation of VcVS signal.

Figure 1 Experimental set up
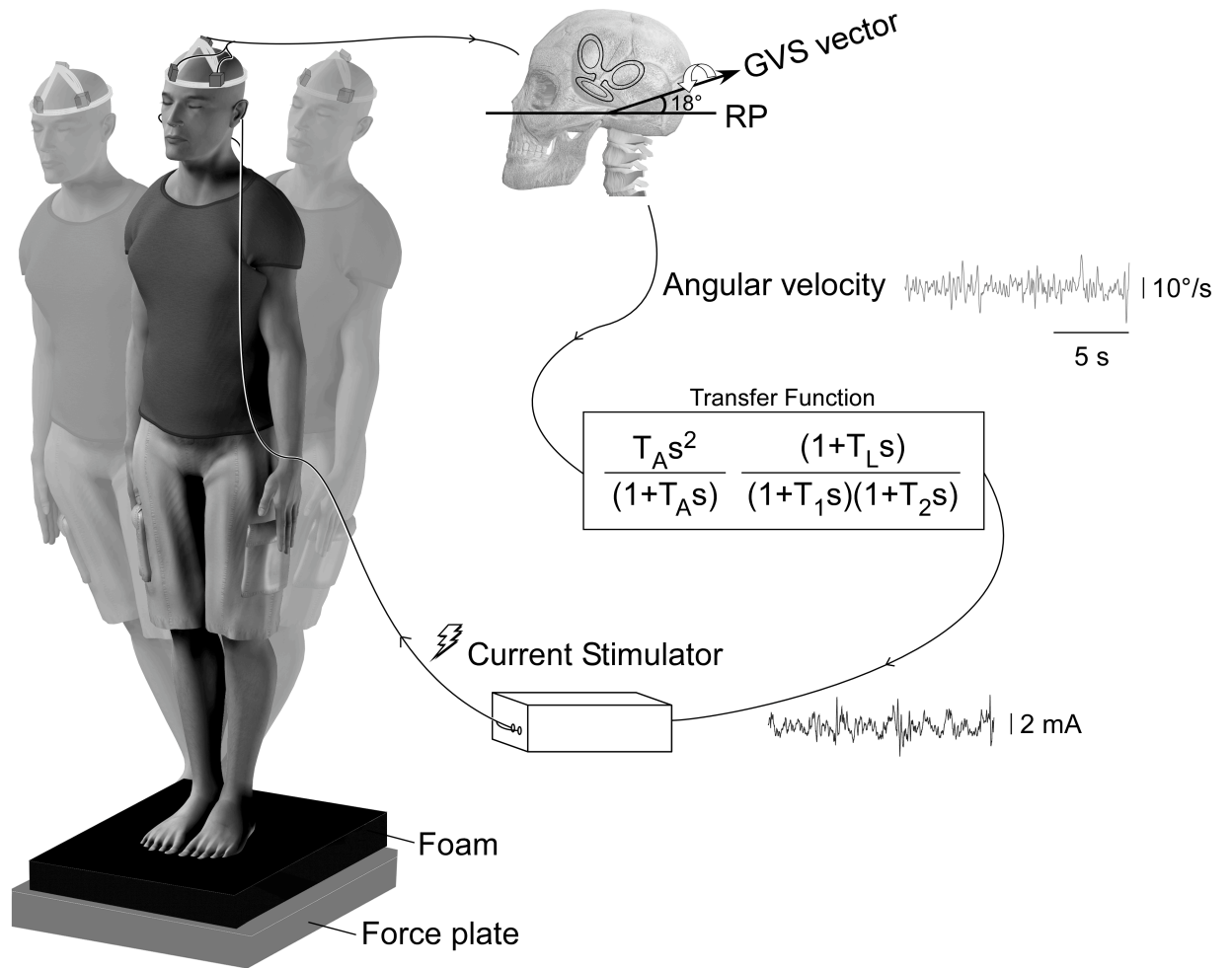
Subjects stood on a foam pad placed on a force plate. The signal from the three angular rate sensors on the head frame was measured relative to the GVS-vector axis and then put through a transfer function to approximate afferent firing rate. The output signal was sent to a current stimulator connected to electrodes on the mastoid processes of the subject. RP: Reid's plane.

Velocity-coupled Vestibular Stimulation (VcVS): Electrical vestibular stimulation evokes a signal of head rotation about the GVS-vector axis, which is directed posteriorly and 18° above Reid's plane (Day & Fitzpatrick, 2005) [top right of Figure 1]. In order to emulate natural vestibular stimulation, the waveform was created to be proportional to instantaneous angular head velocity about the GVS-vector axis. Subjects wore a custom-made head gear with a rigid aluminum frame

aligned in three perpendicular axes, each which supported an angular rate sensor (SDG500, Systron Donner Inertial, Concord, CA, USA) [Figure 2]. Prior to testing, landmarks on the head gear were digitized relative to various anatomic landmarks (nasion, glabella, vertex, occiput, bilateral external auditory meati, mastoid processes, and lower rims of the orbits) with an optoelectronic measurement system (Polaris Vicra, NDI, Waterloo, ON, Canada) [Figure 3]. This procedure determined the position and orientation of the angular rate sensors relative to the GVS vector plane. The instantaneous velocity measured by the angular rate sensors relative to this plane was then passed through the mechanotransduction transfer function described by Fernandez and Goldberg (1971) in order to obtain a signal that was proportional to canal afferent firing rates[6]. This value was then scaled to a factor of ±0.125 mA/°/s to approximate the current intensity used by Day and Reynolds (2005). Using LabVIEW Real-Time (National Instruments, TX, USA), these conversions were computed point-by-point with hierarchal multicore timed structures to ensure conversion rates of 1 ms. Data recorded by the angular rate sensors were lowpass filtered at 100 Hz with an analog filter and sampled at 1000 Hz. The VcVS was computed and generated via a digital-to-analog channel at a rate of 1000 Hz (PXI-8108 with a 18-bit resolution DAQ card (PXI-6289) running LabVIEW 10 and LabVIEW Real-Time, National Instruments, TX, USA).

---

[6] Refer to *Appendix A - Vestibular Transfer Function* for more information

Figure 2 Angular rate sensors on head gear
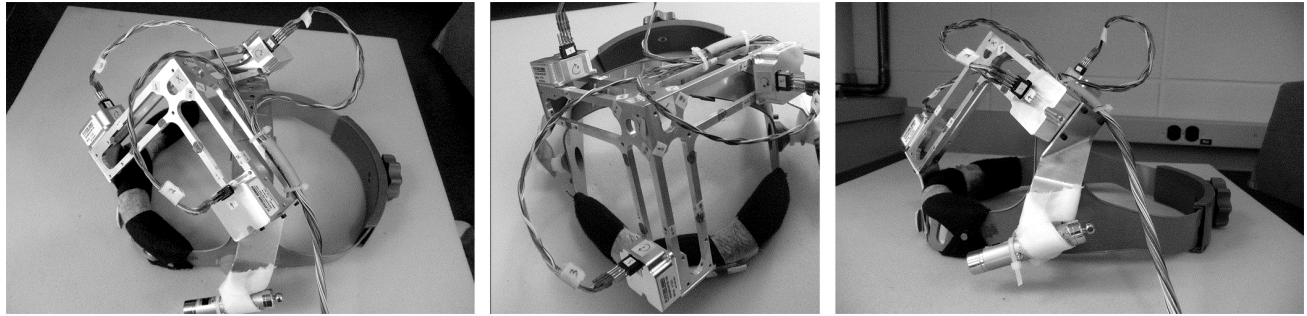
Head gear with rigid head frame supporting angular rate sensors arranged orthogonally.

Figure 3 Digitization of head and headgear landmarks
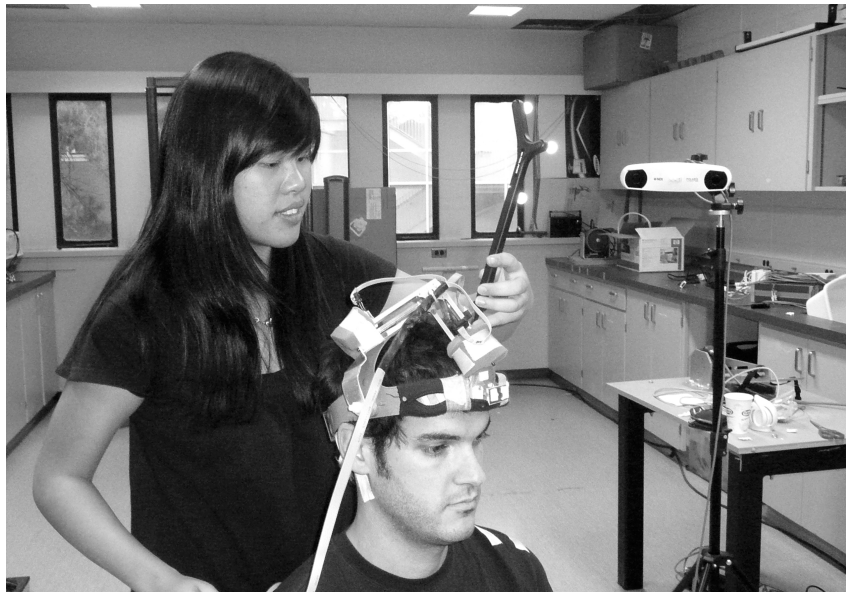
When the electrical stimulus evoked a signal of head rotation in the same direction as real head movement, resulting in a summation of firing frequencies and a signal corresponding to the head moving faster, this was referred to as *additive VcVS*. For instance, for a head roll the right, there is an increase in the afferent discharge on the right side with a corresponding decrease on the left side. With a current of negative polarity (anode left), there would be a further increase in the afferent discharge on the right side and a further decrease on the left side. Conversely, when

the stimulus evoked a signal of head rotation in the opposite direction as real head movement, resulting in a summation of firing frequencies and a signal corresponding to the head moving slower, this was referred to as *subtractive VcVS*. Since the current delivered to the vestibular system was proportional to angular head velocity, the vestibular signal was modulated only during movement. When the head was stationary, minimal current was delivered (root mean square (RMS) amplitude of 0.015 mA).

In Experiment 2, stochastic vestibular stimulation (SVS) was added to VcVS in order to assess modulations in vestibular-induced muscular responses before and after recalibration. SVS has been shown to produce muscular responses with a similar temporal and spatial profile as those evoked by traditional square-wave GVS (Dakin *et al.*, 2007).

Stochastic Vestibular Stimulation (SVS): To elicit vestibular-evoked muscular responses, a SVS signal with a frequency bandwidth of 0-25 Hz and a peak-to-peak amplitude of 2 mA (RMS: 0.54 mA) was added to the VcVS signal (with the limits of ± 9.5 mA maintained) during the pre- and post-test phases. A pilot study was used to identify a peak-to-peak amplitude of 2 mA as the lowest SVS amplitude able to elicit muscular responses in the medial gastrocnemius and tensor fascia latae in all subjects (n=7).

Procedure

For Experiment 1 and 2, subjects stood with their feet together on a 4-inch thick foam pad (Medium density SunMate foam, Columbia Foam Inc, BC, Canada) placed on a force plate (AMTI OR6-7-1000-3985, Advanced Mechanical Technology, Inc., MA, USA). The experimental protocol consisted of three phases for each trial: pre-test, conditioning period and post-test [Figure 4]. The conditioning period involved 240 s (4 min) of VcVS with vision, during which the subjects were asked to make movements with the head in the roll plane, catch and

throw a ball, and perform other simple body movements in the roll plane in order to experience the new vestibular input with visual information. During the pre-test and post-test phases, subjects were instructed to stand, with their eyes closed, facing forward with their head pitched 18° up while they received VcVS for 60 s. For 40 s before and after each trial, subjects stood balanced on the foam with eyes closed and without VcVS.

Figure 4 Experimental protocol
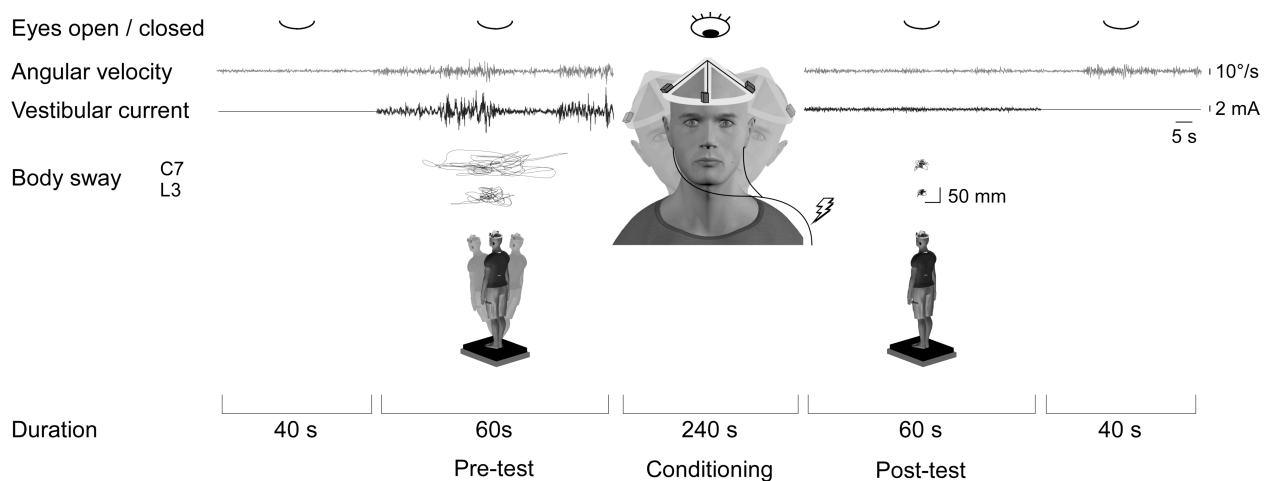
Three phases of each trial were pre-test, conditioning and post-test. During the conditioning phase, subjects had their eyes open and actively moved their head and body in the roll plane. During the pre- and post-test phases, subjects had their eyes closed and were instructed to maintain standing balance. Before the pre-test and after the post-test subjects stood with their eyes closed without stimulation for 40 s. Position sensors were placed at the level of C7 and L3 spinous processes at the midline of the back.

Motion of the body during each trial was measured at the level of the C7 and L3 spinous processes using a three-dimensional motion-tracking system (TrakSTAR, Ascension Technology Corporation, VT, USA) and was sampled at 240 Hz. From these data, the variability of sway amplitude was obtained. Vestibular stimulation, angular rate sensors and force plate data were sampled at 2048 Hz with 18-bit precision (PXI-8108, DAQ card (PXI-6289), National Instruments, TX, USA).

The experimental procedure consisted of four trials. In two of the trials, subjects received either an additive or subtractive VcVS signal. The other two trials served as controls, one with no stimulus (no stimulation control trial) and the other with a pre-recorded signal providing current fluctuations independent of head movement during the conditioning period (non correlated control trial). The pre-recorded signal was the VcVS signal from the conditioning period of either the additive or subtractive VcVS trials; this ensured that the amplitude and frequency composition of the control signal was matched to that experienced during the VcVS trials.

Between each trial, subjects rested seated for a minimum of five minutes to ensure there were no persisting effects of the stimulation from the previous trial. During each trial, an experimenter stood in front of the subject to provide physical support in case balance could not be maintained.

In Experiment 1, five subjects completed an additional trial to assess the ability of the vestibular system to be recalibrated to somatosensory information. During the conditioning period, subjects stepped off the foam and onto a hard surface. The subjects made similar body movements to other conditioning trials but without vision. Subjects stepped up back onto the foam for the post-test phase. All subjects were exposed to the subtractive VcVS for this trial.

In Experiment 2, the SVS signal was added during pre- and post-test periods and each trial was performed twice. Pairs of electrodes (interelectrode distance 2 cm; Ambu Blue Sensors: M type, Ballerup, Denmark) were placed bilaterally over the medial gastrocnemius (r-MG and l-MG) and tensor fascia latae (r-TFL and l-TFL) muscles in order to obtain surface electromyography (EMG) recordings. The skin was thoroughly cleaned with skin preparation gel (NuPrep, D.O. Weaver & Co., Aurora, CO, USA) prior to electrode placement. The EMG signals

were amplified (x1000-10 000), band-pass filtered (10-1000 Hz) (NeuroLog, Digitimer, Hertfordshire, UK) and sampled at 2048 Hz.

Data Reduction

In Experiment 1 and 2, all position data were resolved to the reference frame of the force plate [Figure 5]. The *x*-axis of the reference frame was defined parallel to a line from the center of the force plate to the midpoint of the edge of the force plate and positive left. The *y*-axis was defined parallel to the surface of the force plate perpendicular to the *x*-axis and positive forward. The *z*-axis was positive downward. Medio-lateral (ML) sway occurred about the *y*-axis. Position data were lowpass filtered at 10 Hz with a second order dual-pass Butterworth filter and the standard deviation of the ML sway measured at the levels of C7 and L3 were calculated (Matlab 7.7, Mathworks Inc., MA, USA).

Figure 5 Reference frame

In Experiment 2, the EMG recordings were band-pass filtered at 10-500 Hz with a fourth order dual-pass Butterworth filter and full wave rectified. The EMG data during the pre- and post-test periods were extracted along with the corresponding SVS data. Cumulant density estimates were determined using a modified Matlab code based on the methods of Rosenberg *et al*. (1989). Data from alike trials were concatenated to produce 30 windows generating a frequency resolution of 0.25 Hz (4 s/segment).

Cumulant density estimates, which are described as inverse Fourier transform of the cross spectrum estimate (Brillinger, 1974; Rosenberg *et al.*, 1989), were used to represent the time-domain relationship between SVS and muscle activity. The cumulant density estimate provides a

temporally and spatially similar response to those shown by trigger averaged GVS (Dakin *et al.*, 2007). Cumulant density estimates were normalized by the product of the vector norms of the input (SVS) and output signals (EMG) (Dakin *et al.*, 2010) to account for modulations of muscle responses by background EMG levels (Welgampola & Colebatch, 2001; Lee Son *et al.*, 2008). Because the medium-latency response in the biphasic muscle response is thought to be more functionally relevant for sway (Britton *et al.*, 1993), the peak amplitude of the medium-latency response (beginning approximately at the latency of 100 ms) was extracted for statistical analysis.

Statistical Analysis

In Experiment 1 and 2, to determine whether stimulus type had an impact on sway amplitude during the various phases of the protocol, a two-way repeated measures ANOVA was performed (Statistica, StatSoft, OK, USA). The factors were Time (4 levels) and Stimulus type (4 levels). Fisher's lowest significant difference (LSD) post-hoc tests were used to decompose main effects for stimulus type based on our a priori hypothesis - that the applied vestibular current would increase sway at first and return back to baseline levels after conditioning if the stimulus type was coupled to head movement (additive or subtractive VcVS) and that sway would increase again when the stimulation was turned off to demonstrate the presence of after-effects. To compensate for the eight specific comparisons (comparing sway before and after conditioning as well as the presence of after-effects within each of the four trials), the statistical significance level was reduced to $P < 0.00625$. A simple one-way ANOVA was used to compare sway variability during the pre-test phase with no stimulation of every trial to ensure subjects had returned to baseline values between trials. Statistical significance was set at $P < 0.05$.

For the somatosensory conditioning trial in Experiment 1, a one-way repeated measures ANOVA was performed to determine whether somatosensory information with the absence of

vision during the conditioning period had an impact on sway amplitude during various phases of the protocol. Decomposition of main effects were determined by Fisher's LSD post-hoc tests and to compensate for the two specific comparisons (comparing sway before and after conditioning as well as the presence of after-effects within the trial), statistical significance was reduced to $P < 0.025$.

In Experiment 2, a two way repeated measures ANOVA was used to determine the effect of stimulus type on the peak amplitude of the medium latency response evoked by the SVS (Time (2 levels) × Stimulus type (4 levels)). Decomposition of the main effects for stimulus type was performed using Fisher's LSD post-hoc tests. To compensate for the ten specific comparisons (comparing amplitude before and after conditioning within each of the four trials and comparing all other trials to the control trial between pre and post-test periods), statistical significance was reduced to $P < 0.005$.

Results

All subjects exhibited similar variability in their body sway at both the level of C7 and L3 ($P > 0.05$) prior to the application of the vestibular stimulation[7].

Experiment 1: Body Sway

Body sway was measured before and after conditioning for each of the four trials. When the VcVS was first turned on, all subjects swayed more, often lost balance and 7 of the 8 subjects required external support. Following the conditioning phase, there was a significant reduction in the variability of ML sway in the VcVS trials [Figure 6]. Overall, ML sway variability was reduced by 40 and 34% (at the level of C7 and L3, respectively, Fischer LSD post-hoc, $P < 0.00625$) in the subtractive VcVS trial and reduced by 33 and 32% (at the level of C7 and L3, Fischer LSD post-hoc, $P < 0.00625$) in the additive VcVS trial. In both control trials, differences in the variability of ML sway from pre-test to post-test were not significantly different (Fischer LSD post-hoc, $P > 0.05$).

---

[7] Refer to *Appendix A – Experiment 1 Data and Appendix B – Experiment 2 Data for more information*

Figure 6 Pooled subject data - Exp 1 Sway (recalibration)
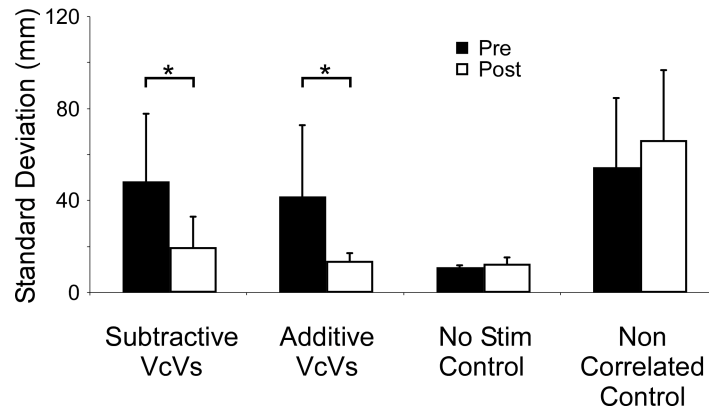
Standard deviation of ML sway from all subjects (n=8) at the level of C7. Statistical analysis showed significant decreases (denoted by *) following the conditioning phase in the subtractive and additive VcVS trials.

Significant after-effects were observed when the stimulus was turned off in the additive VcVS trial [Figure 7]. ML sway variability increased 233 and 111% (at the level of C7 and L3, Fischer LSD post-hoc, $P < 0.00625$) once the VcVS was turned off and subjects still had their eyes closed. The recalibration effects and after-effects on body sway were similar in Experiment 2.

Figure 7 Pooled subject data - Exp 1 Sway (after-effects)
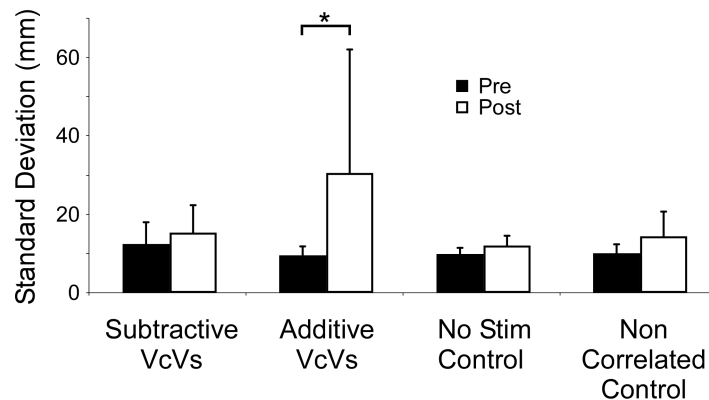
Standard deviation of ML sway from all subjects (n=8) at the level of C7. Statistical analysis showed a significant increase (denoted by *) in ML sway when stimulus was turned off in the additive VcVS trial.

Experiment 1: Somatosensory Conditioning trial

Similar to visual conditioning, ML sway initially increased when the VcVS was turned on and then returned back to baseline levels following somatosensory conditioning. On average, ML sway variability was reduced by 66 and 55% (at the level of C7 and L3, Fischer LSD post-hoc, $P < 0.025$) .

Experiment 2: Electromyographic Responses

Cumulant density estimates were calculated for each muscle in all trials. Figure 8 shows typical EMG responses in the *r*-TFL of one subject. Prior to conditioning, muscular responses in the VcVS and non correlated control trials were attenuated compared to control levels. Following conditioning, the size of the muscular response during the VcVS trials increased to control levels. The size of the response in the non correlated control trial, however, remained considerably smaller. These effects were common across all muscles in all subjects.

Figure 8 Single subject muscular response
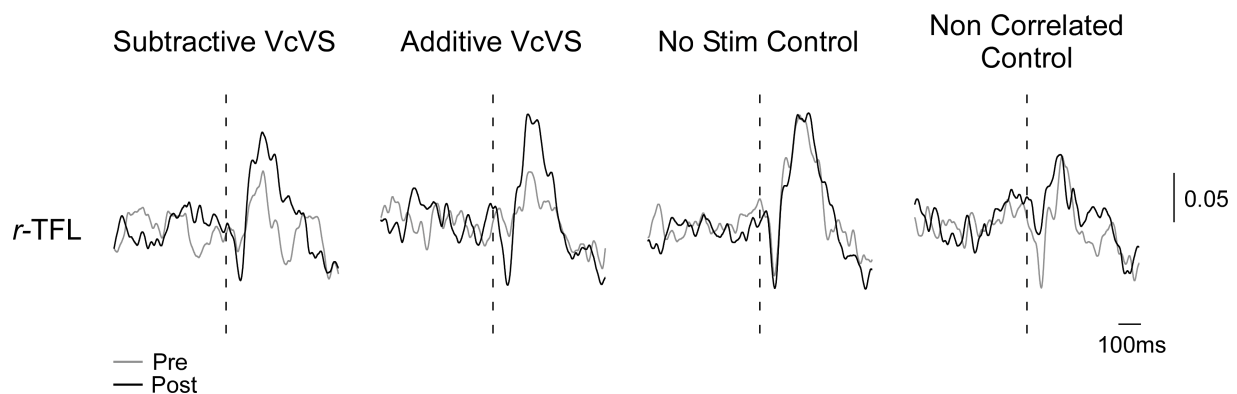
Cumulant density estimates during the pre and post-test for the right tensor fascia latae (r-TFL) for a typical subject. Prior to conditioning, responses in the VcVS and non correlated control trials were smaller than control levels. Following conditioning, the size of the response in the VcVS trials increased to the size of the no stimulation control trial while the non correlated control trial response remained smaller. Dotted line represents 0 ms latency.

In terms of group results [Figure 9] prior to conditioning, the peak amplitudes of both VcVS trials and the non correlated control trial were significantly lower (Fischer LSD, $P < 0.005$) than the no stimulation control trial. After conditioning, the peak amplitude of MG and TFL significantly increased 88 and 77%, respectively, in the subtractive VcVC trial, and 91 and 90%, respectively, in the additive VcVC trial (Fischer LSD post-hoc, $P < 0.005$) and were statistically similar (Fischer LSD post-hoc, $P > 0.05$) to control levels; however, the non correlated control trial remained significantly smaller (Fischer LSD post-hoc, $P < 0.005$).

Figure 9 Pooled subject data - Exp 2 Muscular response - peak amplitude of medium latency response in TFL
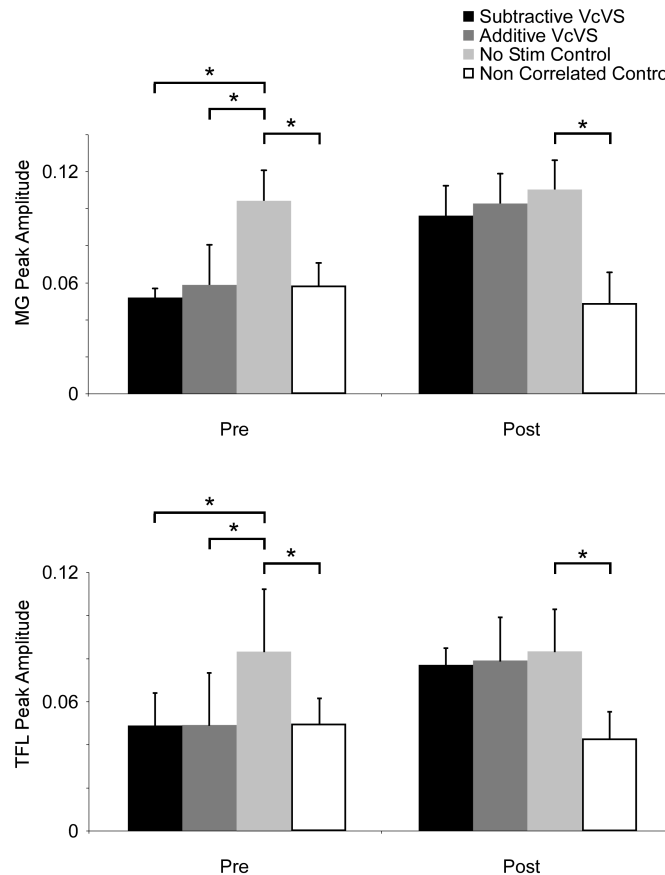
Peak amplitude of the medium latency responses of MG and TFL recordings from all subjects (n=5), Prior to conditioning, the no stimulation control trial was significantly (denoted by *) greater than all other trials. Following conditioning, the peak amplitude in the VcVS trials significantly increased to the same magnitude as the no stimulation control trial. Amplitude of the non correlated control trial did not change.

Discussion

In the present experiments, an initial increase in body sway corresponding to the application of a vestibular stimulus returned to baseline levels after recalibration indicates that a visual signal of head and body motion could recalibrate a vestibular signal indicative of a new head motion. Such recalibration of a new vestibular signal of head motion was associated with an initial decrease followed by an increase in the vestibular-evoked muscular responses, irrespective of the polarity of the VcVS. This finding was contrary to our initial hypothesis but is consistent with findings from literature examining visual and somatosensory recalibration (Lajoie *et al.*, 1992; Jones *et al.*, 2001; Balslev *et al.*, 2004; Bernier *et al.*, 2009).

Recalibration of Vestibular Signal

The effects of visual conditioning on balance during VcVS indicate the gain of the vestibular system can be recalibrated by a reliable visual signal of head rotation. A random vestibular signal, however, cannot be recalibrated. In the control trial where subjects received current fluctuations distinct from head movement, body sway increased at the onset of the stimulus and remained high following the conditioning phase.

With minimal information from other sensory systems, subjects exposed to VcVS misrepresented motion of their head in space and thus, initially had difficulty maintaining balance. During the conditioning phase, subjects used visual information as a reliable reference of head motion to recalibrate the altered vestibular signal. Following this phase, the subject's ability to balance greatly improved, indicating they were interpreting the altered vestibular signal in a different manner. Interestingly, there was an increase in sway variability when the stimulus was turned off. This is akin to the after-effects observed in experiments involving pointing with

prism goggles or moving an arm through a force field (Welch, 1978; Lackner & Dizio, 1994; Shadmehr & Mussa-Ivaldi, 1994) and is considered an indicator of a fundamental change in the interpretation of the stimulus (Shadmehr & Mussa-Ivaldi, 1994). The presence of after-effects also verified that the sensory-motor processes pertaining to maintaining balance were at least partially dependent on incoming vestibular information. However, significant after-effects were seen only in the additive VcVS trial suggesting that vestibular signals of faster head rotation may have been more robustly recalibrated.

When the vestibular system was exposed to a stimulus that was unrelated to head movement, the amount of body sway did not decrease after visual conditioning. Based on these results and contrary to those reported in previous sensory reweighting studies (Day & Cole, 2002; Peterka, 2002; Cenciarini & Peterka, 2006), it can be concluded that the CNS did not decrease the contribution of the vestibular system when it was clearly providing unreliable information. Overall, our results of decreased body sway and after-effects seem to be more in accordance with the sensory fusion hypothesis in that there was a recalibration of the vestibular system by visual signals of head rotation resulting in a unified representation of self-motion with respect to the world (St George & Fitzpatrick, 2010; Ursino *et al.*, 2011).

Somatosensory-vestibular Recalibration

It is well documented that both visual and somatosensory information have large influences on maintaining upright posture (Berthoz *et al.*, 1979; Soechting & Berthoz, 1979; Bles *et al.*, 1984; Straube *et al.*, 1990; Peterka & Benolken, 1995; Redfern *et al.*, 2001). To investigate the idea of somatosensory-vestibular recalibration, five subjects completed a trial in which the conditioning phase consisted of subjects, with eyes closed, making movements in the roll plane while standing on a stable surface to increase proprioceptive information from the feet and

ankles. Similar to the results from visual conditioning trials, subjects experienced a large reduction in sway amplitude variability following somatosensory conditioning indicating that the vestibular system can be recalibrated by various reliable sensory modalities.

Vestibular-evoked Muscular Responses

To examine underlying physiological processes involved in vestibular recalibration, vestibular-evoked muscular responses were investigated in Experiment 2. We compared the magnitude of the muscular response before and after conditioning. The results did not agree with our original hypothesis – that the responses would have divergent changes in magnitude depending on the polarity of the stimulus. Rather, irrespective of whether an additive or subtractive VcVS signal was delivered, the magnitude of the responses were initially reduced and then increased to control levels after recalibration. Conversely, in the non correlated control trial, the muscular responses remained attenuated following conditioning.

From our results, it is apparent that the recalibration process does not occur in the peripheral vestibular system since a random vestibular stimulus evoked a similar muscular response even after the vestibular system was recalibrated. This indicates that the frequency encoding of the vestibular nerves is not recalibrated with respect to head movement. Consequently, a more likely site of the recalibration process would be in the CNS. Specifically, the vestibular nuclei, and the fastigial nucleus and nodulus/uvula of the cerebellum have been associated with processing of vestibular signals arising from self and externally generated head movements (Angelaki & Hess, 1995; Siebold *et al.*, 1997; Roy & Cullen, 2004).

Roy and Cullen (2004) have suggested that vestibular signals arising from self-generated head movements are inhibited by a mechanism that compares expected sensory consequences (efference copy) to actual sensory feedback (re-afference) to dissociate between voluntarily

initiated head movements and unexpected head perturbations. In the present case, because the expected vestibular feedback did not match the actual vestibular feedback prior to conditioning, afferent information arising from the VcVS signal and the SVS signal might have been treated as an externally generated event (ex-afference). As a result, the CNS responded either by: a) down regulating the vestibular signals [Figure 10Ai] or b) by passing the whole stimulus through to be further processed similarly to an unexpected perturbation [Figure 10Bi], the SVS component of which becoming a smaller proportion of the whole signal thereby producing what appears to be an attenuated response. Following conditioning, subjects are able to predict the sensory consequences allowing the efference copy to coincide with sensory re-afference permitting cancelation of the vestibular signals correlated with head movement. Thus, allowing either: a) a return to normal output of vestibular exafferent signals to the muscles [Figure 10Aii] or b) nearly exclusive transmission of the SVS signal [Figure 10Bii] resulting in the magnitude of the muscular responses returning to control levels.

Consistent with the first explanation, an attenuation or absence of proprioceptive feedback has been suggested to be beneficial to tasks that involve sensory conflict as shown in a deafferented patient as well as subjects with temporal proprioceptive deafferentation induced by repetitive transcranial magnetic stimulation (Lajoie *et al.*, 1992; Balslev *et al.*, 2004). Similarly, proprioceptive feedback at the cortical and muscle spindle level have been observed to be decreased during initial stages of visuomotor adaptation (Jones *et al.*, 2001; Bernier *et al.*, 2009). The authors proposed that the reduction in afferent feedback was a strategy for resolving visual and proprioceptive conflict. In the present case, the initial reduction in the magnitude of the muscular responses prior to conditioning could be attributed to a similar neural strategy for resolving sensory conflict.

Figure 10 Discussion models
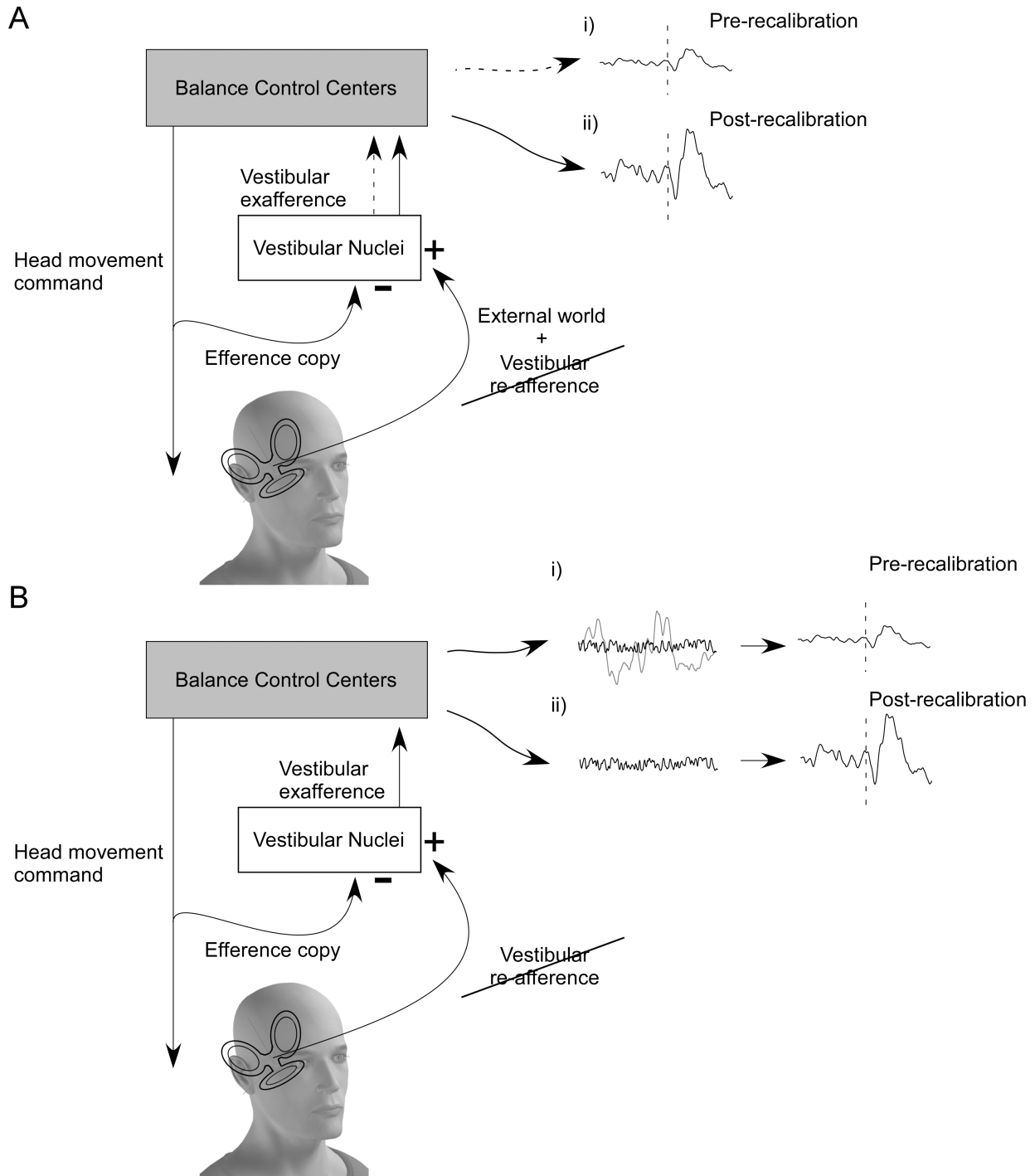
Two different models explaining the results. Ai) Showing the attenuation of the response due to a down regulation (denoted by dotted arrow) of vestibular exafference. Aii) A return of the response to control levels after exafference is no longer suppressed after recalibration. Bi) Attenuation of response due to smaller proportion of SVS in the total exafferent signal. Bii) A return of the response to control levels once velocity-coupled vestibular signals are cancelled resulting in exafferent signal being exclusively SVS.

Conclusions

This study demonstrates that a modified signal of head rotation from the vestibular system is able to be recalibrated by a consistent visual signal. During the initial stages of recalibration, vestibular-evoked muscular responses were reduced, possibly as a neural strategy for resolving sensory discord or as a consequence of the proportion of SVS signal in the uninhibited vestibular signal. Following recalibration, sensory error no longer existed and the transmission of the SVS signal resulted in an increase of the magnitude of the muscular responses to normal levels. Results from the present study suggest that the CNS can control vestibular processes through down regulation or selective gating of vestibular signals to achieve recalibration.

References

Ali AS, Rowen KA & Iles JF. (2003). Vestibular actions on back and lower limb muscles during postural tasks in man. *J Physiol* **546,** 615-624.

Angelaki DE & Cullen KE. (2008). Vestibular system: the many facets of a multimodal sense. *Annu Rev Neurosci* **31,** 125-150.

Angelaki DE & Hess BJ. (1995). Inertial representation of angular motion in the vestibular system of rhesus monkeys. II. Otolith-controlled transformation that depends on an intact cerebellar nodulus. *J Neurophysiol* **73,** 1729-1751.

Angelaki DE, McHenry MQ, Dickman JD, Newlands SD & Hess BJ. (1999). Computation of inertial motion: neural strategies to resolve ambiguous otolith information. *J Neurosci* **19,** 316-327.

Ardic FN, Latt LD & Redfern MS. (2000). Paraspinal muscle response to electrical vestibular stimulation. *Acta Otolaryngol* **120,** 39-46.

Baldissera F, Cavallari P & Tassone G. (1990). Effects of transmastoid electrical stimulation on the triceps brachii EMG in man. *Neuroreport* **1,** 191-193.

Baloh RW & Honrubia V. (2001). *Clinical neurophysiology of the Vestibular System*. Oxford University Press, Toronto.

Balslev D, Christensen LO, Lee JH, Law I, Paulson OB & Miall RC. (2004). Enhanced accuracy in novel mirror drawing after repetitive transcranial magnetic stimulation-induced proprioceptive deafferentation. *J Neurosci* **24,** 9698-9702.

Bear MF, Conners BW & Paradiso MA. (2007). *Neuroscience: exploring the brain*. Lippincott Williams & Wilkins, Baltimore.

Bernier PM, Burle B, Vidal F, Hasbroucq T & Blouin J. (2009). Direct evidence for cortical suppression of somatosensory afferents during visuomotor adaptation. *Cereb Cortex* **19,** 2106-2113.

Berthoz A, Lacour M, Soechting JF & Vidal PP. (1979). The role of vision in the control of posture during linear motion. *Prog Brain Res* **50,** 197-209.

Blanks RH, Curthoys IS & Markham CH. (1975). Planar relationships of the semicircular canals in man. *Acta Otolaryngol* **80,** 185-196.

Bles W, de Jong JM & de Wit G. (1984). Somatosensory compensation for loss of labyrinthine function. *Acta Otolaryngol* **97,** 213-221.

Brillinger DR. (1974). Cross-spectral analysis of processes with stationary increments including the stationary. *Annals of Probability* **2,** 815-827.

Britton TC, Day BL, Brown P, Rothwell JC, Thompson PD & Marsden CD. (1993). Postural electromyographic responses in the arm and leg following galvanic vestibular stimulation in man. *Exp Brain Res* **94,** 143-151.

Carver S, Kiemel T & Jeka JJ. (2006). Modeling the dynamics of sensory reweighting. *Biol Cybern* **95,** 123-134.

Cenciarini M & Peterka RJ. (2006). Stimulus-dependent changes in the vestibular contribution to human postural control. *J Neurophysiol* **95,** 2733-2750.

Dakin CJ, Luu BL, van den Doel K, Inglis JT & Blouin JS. (2010). Frequency-specific modulation of vestibular-evoked sway responses in humans. *J Neurophysiol* **103,** 1048-1056.

Dakin CJ, Son GM, Inglis JT & Blouin JS. (2007). Frequency response of human vestibular reflexes characterized by stochastic stimuli. *J Physiol* **583,** 1117-1127.

Day BL & Cole J. (2002). Vestibular-evoked postural responses in the absence of somatosensory information. *Brain* **125,** 2081-2088.

Day BL & Fitzpatrick RC. (2005). Virtual head rotation reveals a process of route reconstruction from human vestibular signals. *J Physiol* **567,** 591-597.

Day BL, Severac Cauquil A, Bartolomei L, Pastor MA & Lyon IN. (1997). Human body-segment tilts induced by galvanic stimulation: a vestibularly driven balance protection mechanism. *J Physiol* **500 (Pt 3),** 661-672.

Ernst MO & Banks MS. (2002). Humans integrate visual and haptic information in a statistically optimal fashion. *Nature* **415,** 429-433.

Fernandez C & Goldberg JM. (1971). Physiology of peripheral neurons innervating semicircular canals of the squirrel monkey. II. Response to sinusoidal stimulation and dynamics of peripheral vestibular system. *J Neurophysiol* **34,** 661-675.

Fitzpatrick R, Burke D & Gandevia SC. (1994). Task-dependent reflex responses and movement illusions evoked by galvanic vestibular stimulation in standing humans. *J Physiol* **478 (Pt 2),** 363-372.

Fitzpatrick RC & Day BL. (2004). Probing the human vestibular system with galvanic stimulation. *J Appl Physiol* **96,** 2301-2316.

Fredrickson JM, Scheid P, Figge U & Kornhuber HH. (1966). Vestibular nerve projection to the cerebral cortex of the rhesus monkey. *Exp Brain Res* **2,** 318-327.

Goldberg JM & Fernandez C. (1971). Physiology of peripheral neurons innervating semicircular canals of the squirrel monkey. I. Resting discharge and response to constant angular accelerations. *J Neurophysiol* **34,** 635-660.

Goldberg JM, Fernandez C & Smith CE. (1982). Responses of vestibular-nerve afferents in the squirrel monkey to externally applied galvanic currents. *Brain Res* **252,** 156-160.

Goldberg JM, Smith CE & Fernandez C. (1984). Relation between discharge regularity and responses to externally applied galvanic currents in vestibular nerve afferents of the squirrel monkey. *J Neurophysiol* **51,** 1236-1256.

Green AM & Angelaki DE. (2004). An integrative neural network for detecting inertial motion and head orientation. *J Neurophysiol* **92,** 905-925.

Igarashi M. (1967). Dimensional study of the vestibular apparatus. *Laryngoscope* **77,** 1806-1817.

Iles JF & Pisini JV. (1992). Vestibular-evoked postural reactions in man and modulation of transmission in spinal reflex pathways. *J Physiol* **455,** 407-424.

Ivanenko YP, Viaud-Delmon I, Siegler I, Israel I & Berthoz A. (1998). The vestibulo-ocular reflex and angular displacement perception in darkness in humans: adaptation to a virtual environment. *Neurosci Lett* **241,** 167-170.

Jones KE, Wessberg J & Vallbo A. (2001). Proprioceptive feedback is reduced during adaptation to a visuomotor transformation: preliminary findings. *Neuroreport* **12,** 4029-4033.

Jurgens R & Becker W. (2006). Perception of angular displacement without landmarks: evidence for Bayesian fusion of vestibular, optokinetic, podokinesthetic, and cognitive information. *Exp Brain Res* **174,** 528-543.

Kavounoudias A, Gilhodes JC, Roll R & Roll JP. (1999). From balance regulation to body orientation: two goals for muscle proprioceptive information processing? *Exp Brain Res* **124,** 80-88.

Kuhl S, Creem-Regehr S & Thompson W. (2008). Recalibration of rotational locomotion in immersive environments *ACM Transactions on Applied Perceptions* **5,** 1-12.

Lackner JR & Dizio P. (1994). Rapid adaptation to Coriolis force perturbations of arm trajectory. *J Neurophysiol* **72,** 299-313.

Lajoie Y, Paillard J, Teasdale N, Bard C, Fleury M, Forget R & Lamarre Y. (1992). Mirror drawing in a deafferented patient and normal subjects: visuoproprioceptive conflict. *Neurology* **42,** 1104-1106.

Lee Son GM, Blouin JS & Inglis JT. (2008). Short-duration galvanic vestibular stimulation evokes prolonged balance responses. *J Appl Physiol* **105,** 1210-1217.

Lobel E, Kleine JF, Bihan DL, Leroy-Willig A & Berthoz A. (1998). Functional MRI of galvanic vestibular stimulation. *J Neurophysiol* **80,** 2699-2709.

Lobel E, Kleine JF, Leroy-Willig A, Van de Moortele PF, Le Bihan D, Grusser OJ & Berthoz A. (1999). Cortical areas activated by bilateral galvanic vestibular stimulation. *Ann N Y Acad Sci* **871,** 313-323.

Lowenstein O. (1955). The effect of galvanic polarization on the impulse discharge from sense endings in the isolated labyrinth of the thornback ray (Raja clavata). *J Physiol* **127,** 104-117.

Merfeld DM. (1995). Modeling the vestibulo-ocular reflex of the squirrel monkey during eccentric rotation and roll tilt. *Exp Brain Res* **106,** 123-134.

Muller M & Verhagen JH. (1988). A new quantitative model of total endolymph flow in the system of semicircular ducts. *J Theor Biol* **134,** 473-501.

Nashner LM & Wolfson P. (1974). Influence of head position and proprioceptive cues on short latency postural reflexes evoked by galvanic stimulation of the human labyrinth. *Brain Res* **67,** 255-268.

Odkvist LM, Schwarz DW, Fredrickson JM & Hassler R. (1974). Projection of the vestibular nerve to the area 3a arm field in the squirrel monkey (saimiri sciureus). *Exp Brain Res* **21,** 97-105.

Oman CM, Marcus EN & Curthoys IS. (1987). The influence of semicircular canal morphology on endolymph flow dynamics. An anatomically descriptive mathematical model. *Acta Otolaryngol* **103,** 1-13.

Peterka RJ. (2002). Sensorimotor integration in human postural control. *J Neurophysiol* **88,** 1097-1118.

Peterka RJ & Benolken MS. (1995). Role of somatosensory and vestibular cues in attenuating visually induced human postural sway. *Exp Brain Res* **105,** 101-110.

Rabbitt R, Damiano E & Grant J. (2004). *Biomechanics of the semicircular canals and otolith organs*, vol. 19.

Redfern MS, Yardley L & Bronstein AM. (2001). Visual influences on balance. *J Anxiety Disord* **15,** 81-94.

Robinson DA. (1981). The use of control systems analysis in the neurophysiology of eye movements. *Annu Rev Neurosci* **4,** 463-503.

Rosenberg JR, Amjad AM, Breeze P, Brillinger DR & Halliday DM. (1989). The Fourier approach to the identification of functional coupling between neuronal spike trains. *Prog Biophys Mol Biol* **53,** 1-31.

Roy JE & Cullen KE. (2004). Dissociating self-generated from passively applied head motion: neural mechanisms in the vestibular nuclei. *J Neurosci* **24,** 2102-2111.

Shadmehr R & Mussa-Ivaldi FA. (1994). Adaptive representation of dynamics during learning of a motor task. *J Neurosci* **14,** 3208-3224.

Siebold C, Glonti L, Glasauer S & Buttner U. (1997). Rostral fastigial nucleus activity in the alert monkey during three-dimensional passive head movements. *J Neurophysiol* **77,** 1432-1446.

Soechting JF & Berthoz A. (1979). Dynamic role of vision in the control of posture in man. *Exp Brain Res* **36,** 551-561.

Spoor F, Wood B & Zonneveld F. (1994). Implications of early hominid labyrinthine morphology for evolution of human bipedal locomotion. *Nature* **369,** 645-648.

St George RJ & Fitzpatrick RC. (2010). Fusion of sensory channels for the sense of orientation. In *Proceedings of the Physiological Society: Neural processes of orientation and navigation symposium*. United Kingdom.

Steinhausen W. (1933). Uber die beobachtung der cupula in den bogengangsampullen des labyrinths des lebenden hechts. *Pflugers Arch Ges Physiology* **232,** 500-512.

Straube A, Paulus W & Brandt T. (1990). Influence of visual blur on object-motion detection, self-motion detection and postural balance. *Behav Brain Res* **40,** 1-6.

Tortora GJ & Derrickson B. (2006). *Principles of Anatomy and Physiology*. John Wiley & Sons, Hoboken, NJ.

Ursino M, Magosso E & Cuppini C. (2011). Sensory Fusion. In *Perception-Action Cycle: Models, Architectures, and Hardware*, ed. Cutsuridis V, Hussain A & Taylor JG. Springer Science.

van Beers RJ, Sittig AC & Gon JJ. (1999). Integration of proprioceptive and visual position-information: An experimentally supported model. *J Neurophysiol* **81,** 1355-1364.

van der Kooij H, Jacobs R, Koopman B & van der Helm F. (2001). An adaptive model of sensory integration in a dynamic environment applied to human stance control. *Biol Cybern* **84,** 103-115.

Van Egmond AA, Groen JJ & Jongkees LB. (1949). The mechanics of the semicircular canal. *J Physiol* **110,** 1-17.

Viaud-Delmon I, Ivanenko YP, Grasso R & Israel I. (1999). Non-specific directional adaptation to asymmetrical visual-vestibular stimulation. *Brain Res Cogn Brain Res* **7,** 507-510.

Wardman DL, Taylor JL & Fitzpatrick RC. (2003). Effects of galvanic vestibular stimulation on human posture and perception while standing. *J Physiol* **551,** 1033-1042.

Watson SR & Colebatch JG. (1997). EMG responses in the soleus muscles evoked by unipolar galvanic vestibular stimulation. *Electroencephalogr Clin Neurophysiol* **105,** 476-483.

Watson SR & Colebatch JG. (1998). Vestibular-evoked electromyographic responses in soleus: a comparison between click and galvanic stimulation. *Exp Brain Res* **119,** 504-510.

Welch RB. (1978). *Perceptual modification: Adapting to altered sensory environments*. Academic Press, New York.

Welgampola MS & Colebatch JG. (2001). Vestibulospinal reflexes: quantitative effects of sensory feedback and postural task. *Exp Brain Res* **139,** 345-353.

Young LR & Oman CM. (1969). Model for vestibular adaptation to horizontal rotation. *Aerosp Med* **40,** 1076-1080.

Appendix A – Literature Review

Anatomy of the Vestibular System

The human vestibular system provides information to the CNS about static and dynamic movements of the head. There are two main equilibrium-sensing components of the vestibular system: the otolith organs and the semicircular canals (Tortora & Derrickson, 2006). Located in the inner ear and mirror images of each other bilaterally in the head, the vestibular labyrinths are enclosed by a petrous portion of the temporal bones (Baloh & Honrubia, 2001). The entire vestibular structure consists of five receptor organs for equilibrium. The two otolith organs, the saccule and the utricle, detect both static head tilt and linear motion while the three semicircular canals sense head rotation (Bear *et al*., 2007).

The saccule is located on the medial side of the vestibule and is inferior to the utricle. The utricle is oval-shaped and connected to the semicircular canals through five openings (Baloh & Honrubia, 2001). The sensory epithelium of the otoliths is known as the macula which has a surface area of less than 1 mm^2. The two maculae are located perpendicular to each other, vertically-oriented in the saccule and horizontally-oriented in the utricle. The hair cells face opposite directions on either side of a curved portion of the macula, known as the striola (Baloh & Honrubia, 2001). Above the hair cells is a glycoprotein otolithic membrane secreted by long columnar cells interspersed among the hair cells (Tortora & Derrickson, 2006). Over the surface of the membrane are heavy calcium carbonate crystals known as otoconia. Because of their high density, these crystals give a constant downward force of acceleration on the underlying sensory epithelium providing the CNS with a continuous signal of gravity when the head is at rest.

Each of the three semicircular canals has a cross sectional diameter of 0.4 mm and are positioned roughly orthogonal to each other (Baloh & Honrubia, 2001). The horizontal semicircular canal is tilted approximately 30° anteriorly to the transverse plane. The other two

canals are vertically oriented. The anterior semicircular canal is positioned in the medial-lateral plane with the lateral side tilted anteriorly about 45°. Similarly, the posterior semicircular canal is positioned in the medial-lateral plane with the lateral side tilted posteriorly about 45° (Baloh & Honrubia, 2001). There is a bulbous portion known as the ampulla in each semicircular canal which is filled with a fluid known as endolymph. Sensory transduction is caused by mechanical activation of the hair cells by the movement of this fluid (Tortora & Derrickson, 2006). Within the ampulla is an elevated sensory epithelium portion known as the crista. The hair cells are enclosed in a gelatinous material known as the cupula. The fluid in the cupula has the same specific gravity as the endolymph and thus, unlike the otolith organs, there is no constant force applied on the underlying sensory epithelium (Baloh & Honrubia, 2001). In humans, it has been shown that due to evolutionary processes, the anterior and posterior semicircular canals have grown larger and thus, more sensitive compared to the horizontal canal (Oman *et al.*, 1987; Muller & Verhagen, 1988; Spoor *et al.*, 1994). This alteration increases the responsiveness to rotations in the vertical plane.

The hair cells of both the otolith organs and the semicircular canals are connected to first order sensory neurons whose cell bodies lie in Scarpa`s ganglion and make up the vestibular portion of the 8th (vestibulocochlear) cranial nerve which eventually projects onto the vestibular nuclei located in the medulla and pons (Bear *et al.*, 2007).

Physiology and Biomechanics of the Vestibular System

Both the otolith organs and semicircular canals use hair cells as sensory receptors and thus the transduction processes are quite similar. On the apical surface of each hair cell are approximately 70 stereocilia that are arranged from ascending height, the tallest known as a kinocilium (Tortora & Derrickson, 2006). Shear forces applied on the hair cells stretch the

tiplinks that connect the stereocilia and causes mechanically-gated transduction channels to open. The top surface of the hair cell faces endolymph which is rich in potassium whereas the basolateral surface faces perilymph which is rich in sodium (Baloh & Honrubia, 2001). Depending on the direction of the force, the stimulus changes the permeability of various ion channels causing either a depolarization or hyperpolarization of the basolateral membrane which results in an increase or decrease of neurotransmitter released, respectively (Baloh & Honrubia, 2001). If the stereocilia are bent towards the kinocilium, depolarization of the membrane resting potential occurs and excitatory action potentials are produced. Conversely, if the stereocilia are deflected away from the kinocilium, hyperpolarization of the membrane potential occurs and inhibitory potentials are produced. The sensory neurons connected to the hair cells spontaneously fire during rest and any changes due to head motion are merely a modulation of this resting frequency (Goldberg *et al*., 1984) [Figure 11].

Figure 11 Semicircular canal firing
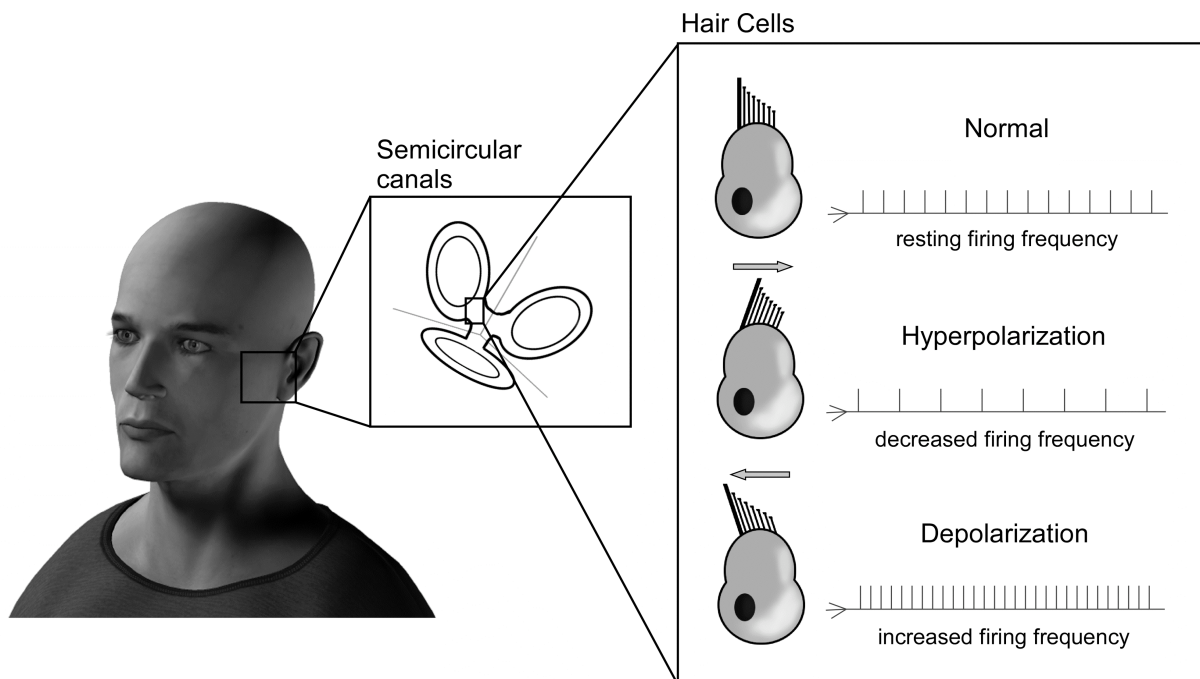
The relation between the direction of of push and the nerve firing frequency.

When the head is level, there is a constant resting force of gravity applied on the hair cells in the maculae of the otolith organs due to the heavy load of the overlying otolithic membrane. When the head is in a static tilt, the otoconia embedded in the otolithic membrane slide the membrane in direction of the tilt and apply a shear force on the hair cells (Bear *et al.*, 2007). Linear head acceleration causes the same transduction signal because as the head moves forward, the otolithic membrane lags behind due to inertia and the hair cells are bent as a result. To differentiate between the two movements, the brain can use information from the semicircular canals to make an internal estimate about the linear acceleration signal that should arise during head tilt relative to gravity. The information that remains from subtracting this signal from the total otolith activation can be interpreted as translational motion (Merfeld, 1995; Angelaki *et al.*, 1999; Green & Angelaki, 2004).

The hair cells located in the crista of the semicircular canals operate in a similar manner to those in the otolith organs. When there is a rotational movement in the head, the endolymph in the canals flow in the opposite direction and push the cupula along with it, causing the hair cells to bend (Baloh & Honrubia, 2001). Analogous to the hair cells in the maculae, bending of the stereocilia leads to opening of ion channels which causes either depolarization or hyperpolarization of the basolateral membrane of the hair cell. Several important differences in the semicircular canals compared to the otolith organs should be noted. Firstly, the fluid in the cupula has a similar density to the surrounding endolymph. Secondly, all the hair cells are oriented in the same direction in the canals compared to otolith organs (Baloh & Honrubia, 2001). Due to the orientation of the semicircular canals, angular motion of the head in any plane can be detected by one or a combination of the canals. Yaw movements are sensed mostly by the horizontal canals whereas the anterior and posterior canals respond to both pitch and roll

movements (Fitzpatrick & Day, 2004). However, prolonged constant angular velocity is not detected by the semicircular canals because after the initial movement of the endolymph, inertial properties of the liquid reinstate and no hair cell transduction occurs (Fitzpatrick & Day, 2004).

The flow of endolymph within the canals faces a large amount of resistance due to the small diameter and large radius of curvature of the semicircular canal. The canal-cupula system resembles a leaky integrator in the physiological mid-frequency range (0.5-4 Hz). Angular acceleration of the head is effectively transduced into an afferent signal which is roughly proportional to angular velocity. Goldberg and Fernandez (1971) have modeled the mechanotransduction as a transfer function that transforms angular acceleration to the approximate afferent firing rate. The angular velocity response is attenuated in high and low frequency ranges because of cupular stiffness and the mass of the endolymph; thus, the canals have been referred to as bandpass angular velocity sensors (Rabbitt *et al*., 2004). A second integration takes place in the brainstem to provide a position signal which is thought to be used by occulomotor neurons to generate the vestibulo-ocular reflex (VOR), a counter rotation of the eyes in response to head movement to maintain a steady retinal image (Robinson, 1981).

Theoretical Frameworks

A primary function of the human vestibular system is to detect the motion of the head and with help of the visual and somatosensory systems, this information allows us to produce appropriate ocular and muscular adjustments to maintain standing balance. The vestibular, visual and somatosensory systems work together to sustain correct body postures essential for everyday life. The integration of overlapping sensory information is thought to contribute to the reliability of our sensory perception of our bodies in space with respect to the world as well as to increase the speed of detecting perturbations and producing appropriate responses. When sensory

discordance arises, illusions and temporary imbalance can occur. Of particular interest are the strategies that the CNS utilizes to solve sensory disagreements to maintain a unified representation of self-orientation.

Traditional research on sensory systems has focused on studying single sense modalities which have provided detailed descriptions on how individual sensory information is coded and processed. Stemming from this research was the idea that discrete senses were received and acted upon by separate and distinct brain areas. Results from current research challenged this idea, clearly showing that the different sensory systems work together and are highly susceptible of influencing each other. Thus, the process of multisensory integration is apparently a much more complex co-operation of the senses, rather than purely a sum of its individual parts (Ursino *et al.*, 2011).

The intricacy of multisensory integration permits a massive range of sensory detection and subsequent motor responses. The primary goal of the CNS is to correctly identify sensations related to the body and the external world and to produce suitable behaviours and reactions. The integration of multisensory information aims to maximize the probability of a correct detection and minimize the possibility of errors. In the case of sensory conflict, the CNS must decide which inputs contribute to the task, and thus included in sensory integration, and which do not, and thus separated (Jurgens & Becker, 2006; Ursino *et al.*, 2011).

Researchers have experimentally induced sensory conflicts in order to study strategies used to resolve sensory disagreement (van Beers *et al.*, 1999; Ernst & Banks, 2002). Regarding standing balance, body sway has been evoked by techniques such as moving visual displays, muscle or tendon vibration, sway-referenced platforms, and electrical stimulation of the vestibular nerves (Watson & Colebatch, 1997; Kavounoudias *et al.*, 1999; Peterka, 2002).

A predominant model that has been suggested to be a strategy of the CNS is *sensory reweighting* (van der Kooij *et al.*, 2001; Carver *et al.*, 2006). This model proposes that the visual, somatosensory and vestibular systems contribute to the representation of the self and the external world. When environmental changes occur, the model predicts that the contribution from unreliable systems are reduced while contribution from other, more relevant systems are concurrently increased in order maintain a relatively stable representation.

Another model that has been recently proposed, known as *sensory fusion*, also suggests that the three sensory systems contribute to the perception of the self and external world (St George & Fitzpatrick, 2010). When sensory conflict arises, instead of changing the contribution of each system, sensory fusion suggests that the systems are recalibrated to the conscious perception of self-motion. There are two main principles regarding the concept of sensory fusion. First, the conscious perception of self-motion determines the reference of recalibration. This perception is constantly changing depending on the availability and agreement of the contributing sensory inputs. The sensory fusion model predicts that if an external error is introduced into one system and not the others, the reafference of all sensory inputs will trigger recalibration to the state that is consciously perceived. The second principle revolves around the idea of maintaining homeostasis. Similar to many physiological systems, a steady state is preferred. A stationary visual field will override podokinetic and vestibular signals whereas a moving visual field shows relatively less dominance.

Galvanic Vestibular Stimulation

Compared to the visual and somatosensory systems, the sense of equilibrium and balance from the vestibular system is more complicated to distort. Previous studies have used virtual

displays and rotation of subjects in space to stimulate the vestibular system (Ivanenko *et al.*, 1998; Viaud-Delmon *et al.*, 1999; Kuhl *et al.*, 2008). One caveat to this type of natural vestibular stimulation is that other confounding sensors are stimulated in parallel and thus, the resultant perceptual or motor adaptation response cannot be purely attributed to the distortion of the vestibular system. Natural vestibular stimulation requires movement of the head in space which unavoidably activates other sensory systems, making it difficult to isolate the influence of the vestibular system. Many researchers investigating postural and myogenic responses have overcome this obstacle by artificially activating the vestibular system by a technique known as GVS (Fitzpatrick & Day, 2004).

Through electrodes placed percutaneously on the mastoid processes of the skull, GVS modulates the firing frequency of the afferent nerves of both the semicircular canals and otolith organs, albeit preferably irregular afferents (Fitzpatrick & Day, 2004). In a bipolar, bilateral configuration, GVS decreases the afferent firing rate on the anodal side and increases the afferent firing rate on the cathodal side in animals (Goldberg *et al.*, 1984) [Figure 12]. From studies on the thornback ray, it has been shown that there is a positive linear relationship between discharge frequency and current stimulus amplitude (Lowenstein, 1955). The site at which GVS acts upon is thought to be the spike trigger zone of the primary afferents, thus bypassing the transduction mechanisms of the vestibular hair cells (Goldberg *et al.*, 1984). In functional magnetic resonance imaging studies on humans, GVS activated regions in the temporoparietal junction, central sulcus and intraparietal sulcus (Lobel *et al.*, 1998; Lobel *et al.*, 1999). In monkeys, these areas in addition to area 3a in the somatosensory cortex and area 2v in the parietal cortex receive vestibular projections and are collectively known as the "vestibular cortex" (Fredrickson *et al.*, 1966; Odkvist *et al.*, 1974).

The brain interprets the GVS current as a real and natural head movement in space produced by movement of the body when in fact, the head remained motionless. Based on the anatomical alignment of the canals and otolith organs (Blanks *et al*., 1975), a vector sum model of GVS has been proposed (Day & Fitzpatrick, 2005). This model predicts the dominant signal that arises from GVS is from the semicircular canals (Day & Cole, 2002; Fitzpatrick & Day, 2004) and the stimulating current evokes a rotational signal around an anterior-posterior axis that is approximately 18° above (posteriorly) to Reid's plane. When GVS is applied in bipolar, bilateral orientation, the subject's response is an illusion of movement if braced or a continuous body sway and tilt towards the anodal side until the movement is stopped by other sensory sources overriding the vestibular signal. The sway response is very sensitive to the parameters such as head and body orientation and availability of information from other sensory systems (Fitzpatrick & Day, 2004). The response is decreased if visual or somatosensory information in available (Britton *et al*., 1993) and is increased by limited somatosensory information such as standing on a foam pad (Fitzpatrick *et al.*, 1994; Wardman *et al.*, 2003) and/or with feet together (Day *et al*., 1997). Vestibular-induced postural responses have been attributed to vestibulo-spinal or vestibulo-reticulo-spinal descending pathways (Baldissera *et al*., 1990; Iles & Pisini, 1992).

Figure 12 Head rotation VS galvanic vestibular stimulation

Head Rotation   Galvanic Vestibular Stimulation
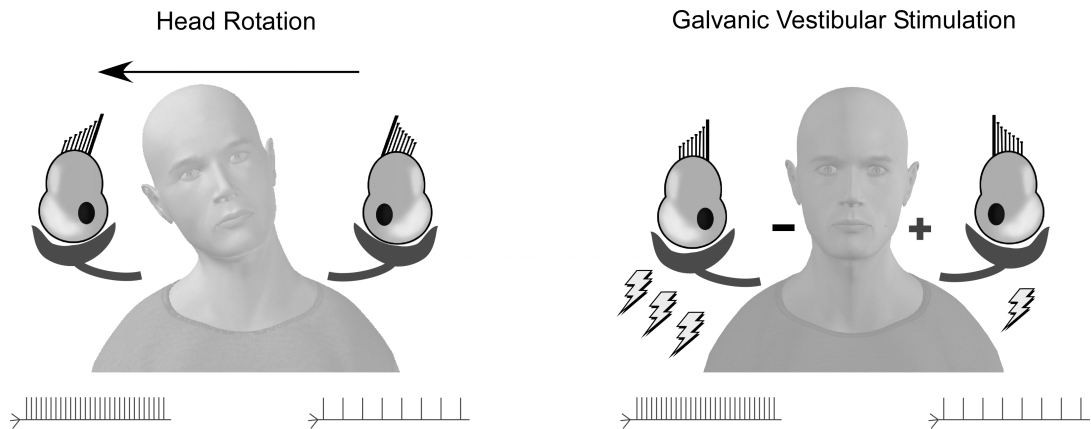
A natural kinetic head rotation (left) causes a similar afferent nerve firing frequency to galvanic vestibular stimulation (right).

GVS-Evoked Muscular Responses

In standing subjects, electrical vestibular stimulation produces characteristic surface EMG responses in muscles that are engaged in the balance task, typically the trunk and limb muscles (Nashner & Wolfson, 1974; Britton *et al.*, 1993; Fitzpatrick *et al.*, 1994; Watson & Colebatch, 1998; Ardic *et al.*, 2000; Ali *et al.*, 2003). The characteristic short- (55-65ms) and medium- (110-120 ms) latency EMG response can be modulated by the intensity and duration of the GVS stimulus as well as by altering sensory inputs such as eye closure or standing on compliant surfaces (Britton *et al.*, 1993; Fitzpatrick *et al.*, 1994; Watson & Colebatch, 1997).

Although most studies have used the traditional square-wave pulses of current to elicit these characteristic muscle responses, Dakin *et al.* (2007) showed that using a stochastic vestibular signal (SVS) induced muscular responses that were spatially and temporally similar to those obtained from trigger averaged GVS. While similar in physiologic effect to GVS, SVS has several advantages over GVS; being more comfortable to the subject, requiring fewer subject

trials as it is a continuous signal, producing a smaller postural response and therefore being less destabilizing than GVS (Dakin *et al.*, 2007; Dakin *et al.*, 2010).

GVS Vector Sum Model

Day and Fitzpatrick (2005) proposed a model to explain the behavioural effects produced by GVS. One assumption is that because GVS is non-directional, the stimulating current is applied to all vestibular afferents equally. When arranged in a bilateral, bipolar arrangement on the mastoid processes of the head, GVS increases the firing rate of all the afferents on the cathodal side and decreases the firing rate on the anodal side (Goldberg *et al*., 1982). Similar to a natural head rotation, this type of afferent firing is interpreted as a yaw movement towards the cathode. The stimulation of the anterior and posterior canals mimics a roll rotation towards the cathodal side. Pitch rotation is cancelled out because the vectors from the anterior and posterior canals are equal and opposite. The resultant vector from the vestibular apparatus is a single vector directed posteriorly and somewhat lateral. The same appears on the contralateral side, thus, the summation of the vectors from both vestibular apparatuses cancels out the lateral components and results in a single vector in the sagittal plane directed posteriorly and anteriorly about 18° above Reid's line [Figure 13].

In the otolith organs, the hair cells are not uniform in directionality. The hair bundles are spread out in a fan-like orientation on the macular surface. When the organs are stimulated electrically, all of the afferents are affected and thus, there is hyperpolarization on one side of the striola and depolarization on the other. This results in a small net acceleration signal because of the small size difference between the inner (pars medialis) and outer (pars lateralis) parts of the utricle but its effects are relatively small when compared to the effects of the semicircular canals (Fitzpatrick & Day, 2004).

Figure 13 GVS vector
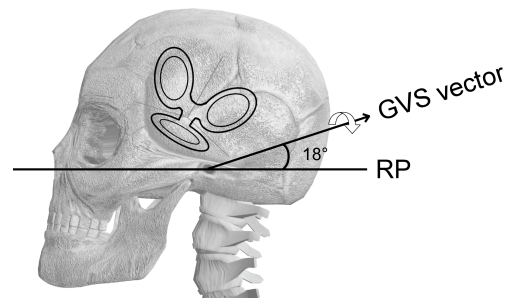
The calculated GVS vector axis is approximately 18° above Reid's plane (RP).

Vestibular Transfer Function

The theory of endolymph flow in semicircular canals was originally thought to be through a narrow canal in which the flow would be stopped by frictional damping in approximately 0.5 s. However, the mechanical properties of the cupula-endolymph system could not explain the subjective reports of sensory after-effects of rotation lasting around 30 s. In 1933, Steinhausen observed that the cupula-endolymph system in the semicircular canals of a pike behaved similarly to a heavily damped, second-order linear system where variables are derived from inertial and damping terms from the mass and viscosity of the endolymph and elastic energy from the cupular structure. The flow of the endolymph did indeed stop after 0.5 s but after-effects were caused by the slow return of the deviated cupula to its original position. Steinhausen's torsion-pendulum model assumes that the discharge of the afferents is proportional to cupular displacement. In 1949, Van Egmond and colleagues (1949), used this model to study human vestibular reactions. It was concluded that the cupula-endolymph system does not act as a pure torsion-pendulum because leaking occurs between the cupula and the ampulla and thus, the discharge rate is not linearly related to cupular displacement. Deviation occurs at both low and high frequencies. At high frequencies (above 1 Hz), there is a gain enhancement as well as a

phase lag. At low frequencies (below 0.0125 Hz), the phase lag is less than expected which was attributed to sensory adaptation (Fernandez & Goldberg, 1971). Young and Oman's (1969) modification to the torsion-pendulum model takes into account the existence of adaptation. The adaptation operator from this equation results in a phase lead at low frequencies and phase lead attenuation at very low frequencies (below 0.0125 Hz).

Fernandez and Goldberg (1971) carried out a series of experiments to investigate the dynamic response of the semicircular canals to angular accelerations (up to $150^{\circ}/s^2$) and sinusoidal stimulation (0.006-8 Hz) in squirrel monkeys (Fernandez & Goldberg, 1971; Goldberg & Fernandez, 1971). Recording electrodes were placed in Scarpa's ganglion and the animals were placed on a rotating platform where the axis of rotation went through the center of the head. These studies led to the development of the following transfer function to approximate the response dynamics which takes into account adaptation and the high frequency lead component.

$$ H(s) = \frac{T_A s}{(1+T_A s)} \frac{(1+T_L s)}{(1+T_1 s)(1+T_2 s)} $$

$H_{TP} = 1/[(1+T_1 s)(1+T_2 s)]$ is the transfer function of torsion-pendulum
$H_A = T_A s/(1+T_A s)$ is the frequency domain representation of the Young-Oman adaptation operator
$H_L = (1+T_L s)$ reproduces the high frequency deviations from the torsion pendulum model, including gain enhancement and progressive phase lead
$T_1 = \Pi/\Delta$ from original torsion-pendulum model
$T_2 = \Theta/\Pi$ from original torsion-pendulum model

Fernandez and Goldberg's mechanotransduction transfer function predicted the physiological data more accurately compared to the torsion-pendulum model especially at low and high frequencies. The transfer function requires the estimation of four time constants T_1, T_2, T_A, and T_L. From primate data, these were found to be 5.7 s, 0.003 s, 80 s and 0.049 s, respectively.

Appendix B – Experiment 1 Data

Table 1 Subject data - Exp 1 Sway (recalibration)

Sway Variability Data (mm) - Stim On

Trial	Subject	Position Sensor C7		Position Sensor L3	
		Pre	**Post**	**Pre**	**Post**
Subtractive VcVS	1	51.57	14.08	15.15	10.18
	2	80.77	11.41	39.37	7.68
	3	71.74	12.75	24.03	7.27
	4	10.77	14.02	8.30	8.65
	5	21.05	14.97	10.84	7.99
	6	40.96	9.78	21.38	6.96
	7	16.61	22.68	11.14	15.96
	8	86.86	51.85	58.77	32.70
	Mean(SD)	**47.54(30.02)**	**18.94(13.83)**	**23.62(17.38)**	**12.17(8.79)**
Additive VcVS	1	63.07	12.93	18.06	8.13
	2	85.56	8.93	32.39	6.27
	3	63.97	8.11	21.01	4.52
	4	11.61	8.90	9.43	6.64
	5	13.29	14.95	8.18	7.87
	6	9.73	16.48	8.13	11.96
	7	65.33	15.65	35.32	10.06
	8	15.64	17.69	11.22	12.85
	Mean(SD)	**41.02(31.27)**	**12.95(3.82)**	**17.97(10.88)**	**8.54(2.88)**
No Stim Control	1	11.60	12.97	6.94	8.67
	2	8.83	12.92	6.56	8.92
	3	10.24	8.23	5.14	4.73
	4	9.28	9.31	6.30	6.44
	5	9.38	13.36	5.12	6.95
	6	9.02	9.16	6.76	6.36
	7	9.97	10.24	7.17	7.49
	8	13.11	18.08	9.31	12.79
	Mean(SD)	**10.18(1.48)**	**11.78(3.23)**	**6.66(1.23)**	**7.79(2.27)**
Non Correlated Control	1	101.70	103.55	37.01	33.04
	2	65.90	102.69	27.95	47.04
	3	64.46	56.46	18.43	21.14
	4	15.54	34.02	10.68	19.85
	5	13.52	51.97	7.41	23.80
	6	35.61	23.22	19.84	14.34
	7	73.32	90.85	51.33	63.04
	8	61.15	62.93	39.49	42.09
	Mean(SD)	**53.90(30.25)**	**65.71(30.53)**	**26.52(15.22)**	**33.04(16.60)**

Table 2 Subject data - Exp 1 Sway (after-effects)

Sway Variability Data (mm) - Stim Off

Trial	Subject	Position Sensor C7		Position Sensor L3	
		Pre	**Post**	**Pre**	**Post**
Subtractive VcVS	1	7.99	13.45	5.51	7.13
	2	10.38	24.53	6.36	14.29
	3	8.20	9.17	4.40	4.49
	4	23.14	8.37	13.01	5.54
	5	8.38	9.89	4.57	4.95
	6	6.96	25.22	5.59	13.77
	7	13.49	8.04	9.89	5.99
	8	17.86	19.97	12.80	13.70
Mean(SD)		**12.05(5.76)**	**14.83(7.32)**	**7.77(3.60)**	**8.73(4.37)**
Additive VcVS	1	7.60	103.01	5.28	27.00
	2	13.01	43.56	8.28	19.76
	3	7.95	13.29	4.09	6.76
	4	6.05	7.48	4.15	5.30
	5	7.66	15.42	4.92	7.83
	6	7.26	30.73	6.13	20.73
	7	10.52	14.83	8.03	9.75
	8	12.08	12.19	9.37	8.92
Mean(SD)		**9.02(2.52)**	**30.06(31.76)**	**6.28(2.03)**	**13.26(8.05)**
No Stim Control	1	12.02	9.86	7.11	6.60
	2	8.62	13.38	5.77	8.93
	3	10.71	8.76	6.30	4.76
	4	8.07	11.73	6.22	8.35
	5	10.00	9.79	5.74	5.47
	6	6.19	10.25	4.64	7.42
	7	9.36	12.65	6.64	8.09
	8	10.33	17.12	8.12	12.15
Mean(SD)		**9.41(1.79)**	**11.69(2.70)**	**6.32(0.96)**	**7.72(2.15)**
Non Correlated Control	1	14.36	13.29	7.71	8.04
	2	10.70	24.11	7.36	11.88
	3	8.22	9.35	4.41	4.97
	4	6.23	5.49	4.93	4.42
	5	8.08	13.93	5.17	7.50
	6	7.41	8.64	5.21	6.50
	7	10.14	13.57	7.52	8.84
	8	11.43	23.06	9.11	13.06
Mean(SD)		**9.57(2.61)**	**13.93(6.63)**	**6.43(1.70)**	**8.15(3.06)**

Table 3 Subject data - Exp 1 Trunk-lumbar roll

Trunk - lumbar roll (degrees)

Trial	Subject	Stim On		Stim Off	
		Pre	**Post**	**Pre**	**Post**
Subtractive VcVS	1	2.21	0.89	0.61	0.59
	2	1.80	0.63	0.35	0.76
	3	2.65	0.47	0.27	0.64
	4	0.24	0.32	0.26	0.22
	5	0.52	0.32	0.38	0.33
	6	0.90	0.28	0.17	1.42
	7	0.48	1.15	0.21	0.30
	8	2.52	1.43	0.36	0.54
	Mean(SD)	**1.42(0.99)**	**0.69(0.43)**	**0.33(0.14)**	**0.60(0.38)**
Additive VcVS	1	3.40	0.85	0.53	2.91
	2	2.91	0.46	0.39	1.94
	3	2.00	0.34	0.30	0.50
	4	0.24	0.28	0.34	0.52
	5	0.50	0.36	0.20	0.35
	6	0.31	0.33	0.18	0.68
	7	1.70	0.29	0.36	0.24
	8	0.39	0.30	0.33	0.23
	Mean(SD)	**1.43(1.26)**	**0.40(0.19)**	**0.31(0.12)**	**0.86(0.93)**
No Stim Control	1	0.55	0.74	0.65	0.65
	2	0.24	0.58	0.23	0.38
	3	0.25	0.39	0.34	0.26
	4	0.21	0.35	0.17	0.22
	5	0.20	0.23	0.16	0.20
	6	0.20	0.17	0.17	0.41
	7	0.22	0.37	0.15	0.30
	8	0.32	0.48	0.18	0.23
	Mean(SD)	**0.27(0.12)**	**0.42(0.18)**	**0.26(0.17)**	**0.33(0.15)**
Non Correlated Control	1	3.09	2.50	0.66	0.74
	2	2.04	4.13	0.34	1.90
	3	4.64	4.58	0.28	1.23
	4	0.32	0.79	0.29	0.33
	5	0.45	1.28	0.38	0.38
	6	0.69	0.61	0.15	0.20
	7	1.54	1.78	0.29	0.42
	8	1.47	1.81	0.16	0.59
	Mean(SD)	**1.78(1.38)**	**2.19(1.38)**	**0.32(0.16)**	**0.72(0.57)**

Table 4 Subject data - Exp 1 Somatosensory conditioning (recalibration)

Sway Variability Data (mm) - Stim On

Trial	Subject	Position Sensor C7		Position Sensor L3	
		Pre	**Post**	**Pre**	**Post**
Somatosensory Conditioning	1	102.46	11.55	39.97	6.46
	2	73.98	13.37	36.24	9.14
	3	61.39	18.72	21.71	9.22
	4	31.76	13.52	11.64	8.07
	5	26.70	17.89	15.63	11.42
	Mean(SD)	**59.26(31.24)**	**15.01(3.12)**	**25.04(12.53)**	**8.86(1.81)**

Table 5 Subject data - Exp 1 Somatosensory conditioning (after-effects)

Sway Variability Data (mm) - Stim Off

Trial	Subject	Position Sensor C7		Position Sensor L3	
		Pre	**Post**	**Pre**	**Post**
Somatosensory Conditioning	1	13.07	18.15	7.20	9.74
	2	12.72	76.57	9.18	24.58
	3	13.38	24.26	6.02	10.07
	4	10.07	11.68	6.18	7.27
	5	8.71	24.72	6.33	15.37
	Mean(SD)	**11.59(2.08)**	**31.08(25.98)**	**6.98(1.31)**	**13.41(6.91)**

Appendix C – Experiment 2 Data

Table 6 Subject data - Exp 2 Sway (recalibration)

Sway Variability Data (mm) - Stim On

Trial	Subject	Position Sensor C7		Position Sensor L3	
		Pre	**Post**	**Pre**	**Post**
Subtractive VcVS	1	85.82	24.66	44.33	15.60
	2	67.18	29.43	39.25	18.79
	3	83.09	33.09	50.43	20.24
	4	54.33	42.06	29.01	21.43
	5	55.93	22.18	39.45	14.98
	Mean(SD)	**69.27(14.75)**	**30.28(7.82)**	**40.50(7.87)**	**18.21(2.83)**
Additive VcVS	1	92.78	12.69	40.50	8.57
	2	52.09	17.53	26.81	12.07
	3	65.41	16.72	41.53	11.07
	4	55.55	31.87	23.47	14.13
	5	17.19	11.82	12.00	8.71
	Mean(SD)	**56.60(27.21)**	**18.13(8.07)**	**28.86(12.38)**	**10.91(2.35)**
No Stim Control	1	24.15	16.22	15.02	10.15
	2	20.44	22.69	12.66	14.53
	3	22.32	19.05	13.95	11.76
	4	17.05	19.77	8.27	9.81
	5	15.89	21.34	11.20	13.85
	Mean(SD)	**19.97(3.48)**	**19.82(2.45)**	**12.22(2.63)**	**12.02(2.13)**
Non Correlated Control	1	77.34	97.51	40.95	46.35
	2	85.15	88.93	47.97	51.19
	3	79.50	86.15	48.29	48.99
	4	67.98	65.83	37.39	32.74
	5	49.86	58.44	30.24	24.70
	Mean(SD)	**71.97(13.82)**	**79.37(16.49)**	**40.97(7.59)**	**40.79(11.51)**

Table 7 Subject data - Exp 2 Sway (after-effects)

Sway Variability Data (mm) - Stim Off

Trial	Subject	Position Sensor C7		Position Sensor L3	
		Pre	**Post**	**Pre**	**Post**
Subtractive VcVS	1	11.61	22.50	8.20	12.61
	2	12.56	39.94	8.77	23.72
	3	9.23	26.87	6.23	16.65
	4	9.52	28.57	5.96	17.68
	5	10.50	13.52	8.17	9.42
	Mean(SD)	**10.68(1.41)**	**26.28(9.61)**	**7.47(1.28)**	**16.02(5.42)**
Additive VcVS	1	11.15	51.95	8.22	25.95
	2	14.97	49.02	10.64	27.37
	3	8.67	30.87	6.06	13.97
	4	9.18	15.55	5.96	8.63
	5	9.19	10.19	7.29	7.50
	Mean(SD)	**10.63(2.61)**	**31.51(18.93)**	**7.63(1.92)**	**16.68(9.44)**
No Stim Control	1	13.03	15.92	9.43	11.29
	2	16.19	18.35	10.26	12.26
	3	9.93	11.71	7.18	7.69
	4	12.57	14.10	7.17	8.15
	5	10.79	11.80	8.23	8.35
	Mean(SD)	**12.50(2.42)**	**14.38(2.83)**	**8.45(1.37)**	**9.55(2.08)**
Non Correlated Control	1	11.17	15.76	8.08	10.30
	2	15.85	20.73	9.68	14.47
	3	10.87	11.59	7.02	7.46
	4	11.20	9.08	6.34	5.51
	5	9.14	9.80	7.09	7.02
	Mean(SD)	**11.64(2.50)**	**13.39(4.86)**	**7.64(1.30)**	**8.95(3.54)**

Table 8 Subject data - Exp 2 Muscular response - peak amplitude of medium latency response (normalized)

Peak amplitude of medium latency response

Trial	Subject	TFL(10^2)		MG(10^2)		All EMG(10^2)	
		Pre	**Post**	**Pre**	**Post**	**Pre**	**Post**
Subtractive VcVS	1	3.95	8.35	4.61	11.59	4.28	9.97
	2	3.61	5.72	4.75	7.09	4.18	6.41
	3	6.33	8.14	5.62	9.00	5.97	8.57
	4	3.37	6.93	4.85	10.12	4.11	8.53
	5	6.72	7.42	5.87	10.13	6.30	8.77
	Mean(SD)	**4.80(1.60)**	**7.31(1.05)**	**5.14(0.56)**	**9.58(1.67)**	**4.97(1.07)**	**8.45(1.29)**
Additive VcVS	1	3.44	9.71	4.36	12.66	3.90	11.18
	2	2.03	5.83	4.07	8.08	3.05	6.96
	3	6.44	9.43	4.97	9.69	5.70	9.56
	4	4.35	5.49	6.41	10.70	5.38	8.09
	5	8.20	8.92	9.43	9.97	8.82	9.45
	Mean(SD)	**4.89(2.45)**	**7.88(2.05)**	**5.85(2.20)**	**10.22(1.67)**	**5.37(2.21)**	**9.05(1.60)**
No Stim Control	1	5.20	7.58	9.04	11.97	7.12	9.78
	2	5.86	5.87	8.41	8.38	7.13	7.13
	3	12.12	11.34	10.38	12.20	11.25	11.77
	4	8.27	8.21	12.68	11.96	10.48	10.09
	5	10.13	8.56	11.26	10.43	10.70	9.49
	Mean(SD)	**8.32(2.90)**	**8.31(1.98)**	**10.36(1.72)**	**10.99(1.62)**	**9.34(2.04)**	**9.65(1.67)**
Non Correlated Control	1	4.77	2.55	5.13	3.07	4.95	2.81
	2	3.34	3.52	5.24	3.56	4.29	3.54
	3	5.06	3.96	4.39	4.22	4.72	4.09
	4	4.54	5.46	6.23	7.09	5.39	6.28
	5	6.80	5.65	7.83	6.20	7.31	5.93
	Mean(SD)	**4.90(1.24)**	**4.23(1.32)**	**5.76(1.33)**	**4.83(1.74)**	**5.33(1.17)**	**4.53(1.51)**

Figure 14 Pooled subject data - Exp 2 Muscular response - peak amplitude of medium latency response in TFL, MG and combined EMG (normalized)
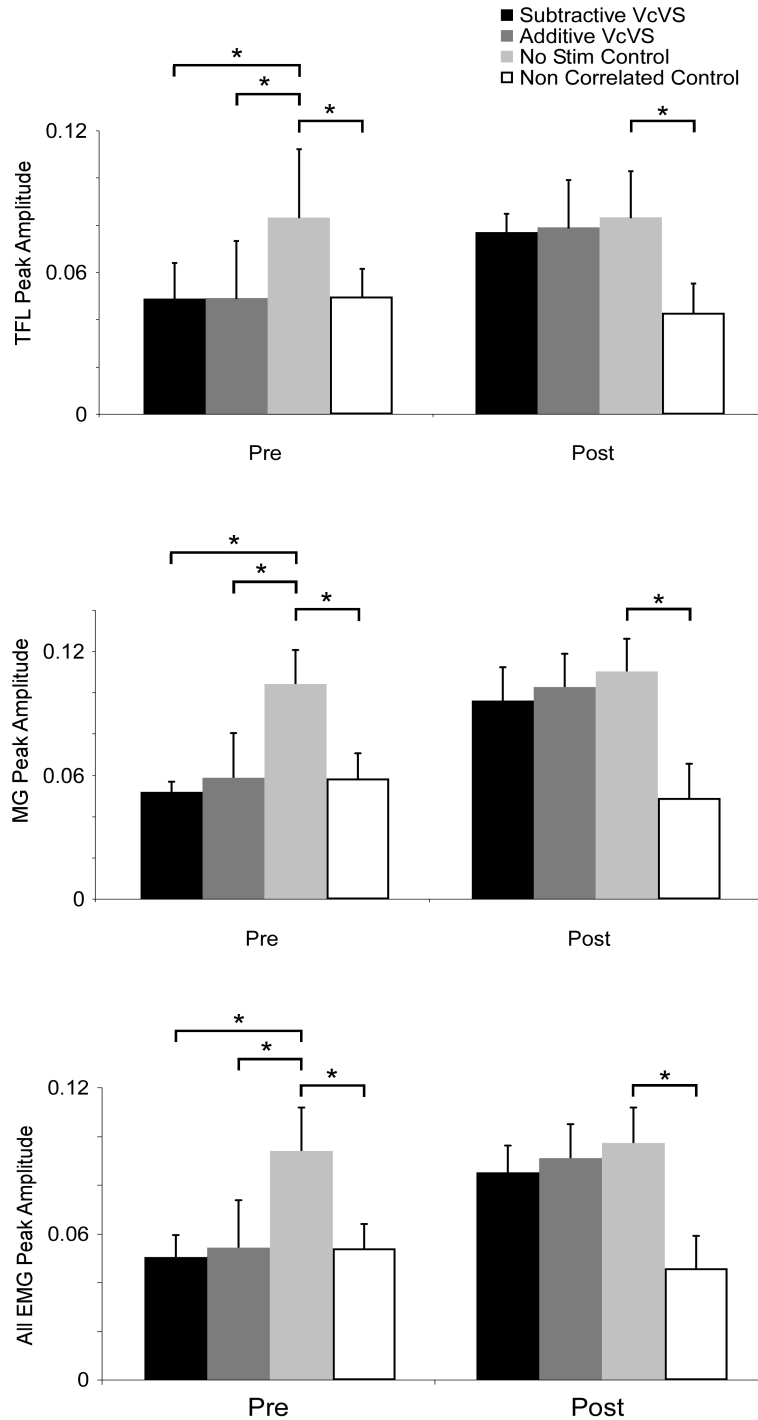

Peak amplitude of the medium latency responses (normalized for background EMG) of TFL, MG and combined EMG recordings from all subjects (n=5), (Fischer's LSD, P < 0.005; significance denoted by (*)).

Table 9 Subject data - Exp 2 Muscular response - magnitude of medium latency response (normalized)

Magnitude of first 120 ms of medium latency response

Trial	Subject	TFL		MG		All EMG	
		Pre	**Post**	**Pre**	**Post**	**Pre**	**Post**
Subtractive VcVS	1	6.45	14.09	7.93	17.70	7.19	15.90
	2	6.13	9.46	6.79	11.53	6.46	10.49
	3	11.13	15.30	9.83	14.82	10.48	15.06
	4	5.04	11.64	7.71	17.96	6.37	14.80
	5	9.77	14.15	9.63	17.06	9.70	15.61
	Mean(SD)	**7.70(2.61)**	**12.93(2.36)**	**8.38(1.31)**	**15.81(2.70)**	**8.04(1.92)**	**14.37(2.21)**
Additive VcVS	1	5.71	16.34	7.15	19.22	6.43	17.78
	2	2.25	8.09	4.89	14.28	3.57	11.19
	3	9.93	17.51	8.45	17.34	9.19	17.43
	4	6.98	8.84	9.96	17.19	8.47	13.02
	5	13.36	17.18	15.71	17.73	14.53	17.45
	Mean(SD)	**7.64(4.22)**	**13.59(4.71)**	**9.23(4.07)**	**17.15(1.80)**	**8.44(4.05)**	**15.37(3.06)**
No Stim Control	1	8.38	12.99	14.90	18.45	11.64	15.72
	2	9.33	8.59	14.81	13.90	12.07	11.24
	3	20.87	20.83	18.77	21.04	19.82	20.93
	4	14.40	14.00	22.38	22.69	18.39	18.34
	5	16.53	15.57	21.24	18.32	18.89	16.95
	Mean(SD)	**13.90(5.17)**	**14.40(4.43)**	**18.42(3.51)**	**18.88(3.34)**	**16.16(3.97)**	**16.64(3.58)**
Non Correlated Control	1	7.26	3.81	8.25	4.51	7.76	4.16
	2	5.37	6.29	7.42	5.46	6.40	5.88
	3	8.18	5.58	7.52	6.71	7.85	6.15
	4	7.20	8.20	10.10	11.27	8.65	9.73
	5	12.14	9.89	13.28	9.15	12.71	9.52
	Mean(SD)	**8.03(2.51)**	**6.75(2.35)**	**9.31(2.46)**	**7.42(2.77)**	**8.67(2.40)**	**7.09(2.44)**

Figure 15 Pooled subject data - Exp 2 Muscular response - magnitude of 120 ms of medium latency response in TFL, MG and combined EMG (normalized)
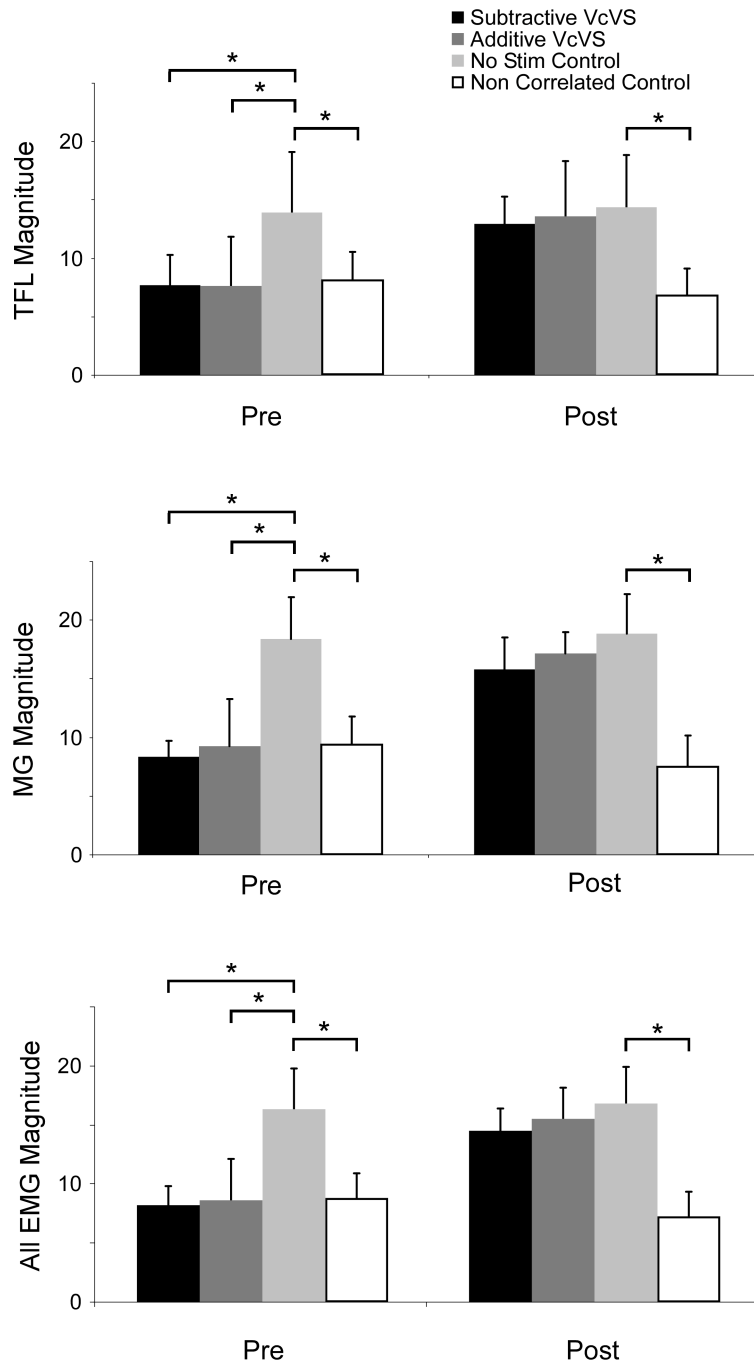

Magnitude of 120 ms of the medium latency responses (normalized for background EMG) of TFL, MG and combined EMG recordings from all subjects (n=5), (Fischer's LSD, P < 0.005; significance denoted by (*)).

Table 10 Subject data - Exp 2 Muscular response - peak amplitude of medium latency response (non normalized)

Peak amplitude of medium latency response

Trial	Subject	TFL(10^2)		MG(10^2)		All EMG(10^2)	
		Pre	**Post**	**Pre**	**Post**	**Pre**	**Post**
Subtractive VcVS	1	0.41	0.71	0.19	0.44	0.30	0.57
	2	0.39	0.55	0.46	0.57	0.43	0.56
	3	1.29	1.27	0.24	0.35	0.76	0.81
	4	0.42	0.96	0.18	0.35	0.30	0.65
	5	1.12	0.79	0.13	0.20	0.62	0.49
	Mean(SD)	**0.73(0.44)**	**0.86(0.27)**	**0.24(0.13)**	**0.38(0.14)**	**0.48(0.20)**	**0.62(0.12)**
Additive VcVS	1	0.35	0.82	0.17	0.45	0.26	0.63
	2	0.19	0.43	0.41	0.59	0.30	0.51
	3	1.16	1.33	0.21	0.36	0.68	0.85
	4	0.80	0.67	0.27	0.37	0.53	0.52
	5	0.78	0.74	0.16	0.20	0.47	0.47
	Mean(SD)	**0.66(0.39)**	**0.80(0.33)**	**0.24(0.10)**	**0.39(0.14)**	**0.45(0.17)**	**0.60(0.15)**
No Stim Control	1	0.30	0.42	0.26	0.36	0.28	0.39
	2	0.34	0.40	0.63	0.63	0.48	0.51
	3	1.35	1.07	0.40	0.42	0.88	0.75
	4	0.86	0.42	0.48	0.38	0.67	0.40
	5	0.87	0.79	0.21	0.20	0.54	0.50
	Mean(SD)	**0.75(0.43)**	**0.62(0.30)**	**0.40(0.17)**	**0.40(0.15)**	**0.57(0.22)**	**0.51(0.14)**
Non Correlated Control	1	0.52	0.24	0.18	0.11	0.35	0.18
	2	0.34	0.38	0.48	0.33	0.41	0.36
	3	0.72	0.52	0.17	0.14	0.44	0.33
	4	0.98	0.93	0.27	0.25	0.63	0.59
	5	0.91	0.78	0.15	0.10	0.53	0.44
	Mean(SD)	**0.70(0.27)**	**0.57(0.28)**	**0.25(0.14)**	**0.19(0.10)**	**0.47(0.11)**	**0.38(0.15)**

Figure 16 Pooled subject data - Exp 2 Muscular response - peak amplitude of medium latency response in TFL, MG and combined EMG (non normalized)
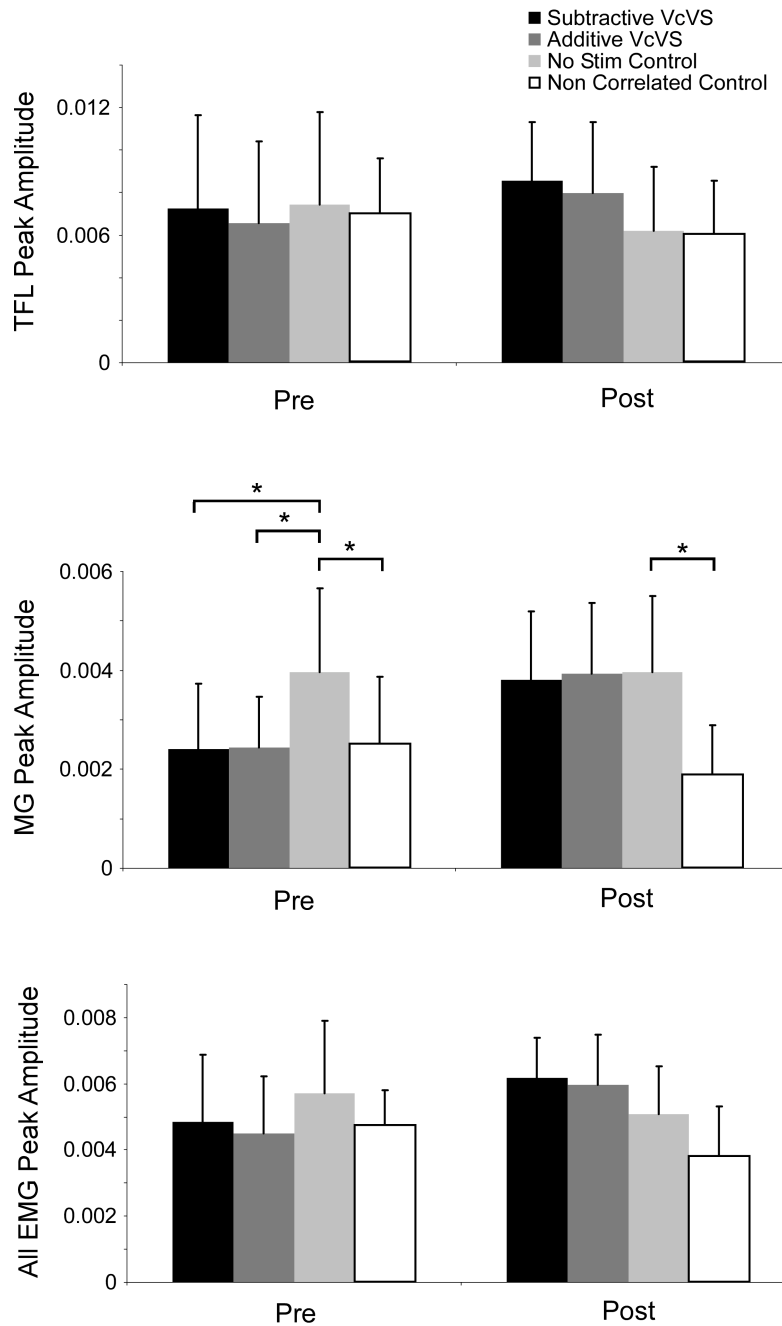

Peak amplitude of the medium latency responses (non normalized for background EMG) of TFL, MG and combined EMG recordings from all subjects (n=5), (Fischer's LSD, P < 0.005; significance denoted by (*)).

Table 11 Subject data - Exp 2 Muscular response - magnitude of medium latency response (non normalized)

Magnitude of first 120 ms of medium latency response

Trial	Subject	TFL		MG		All EMG	
		Pre	**Post**	**Pre**	**Post**	**Pre**	**Post**
Subtractive VcVS	1	67.34	119.99	33.46	66.36	50.40	93.18
	2	66.69	91.71	66.46	94.18	66.57	92.94
	3	226.13	238.54	42.33	57.56	134.23	148.05
	4	64.72	165.65	28.39	62.89	46.56	114.27
	5	162.81	149.99	20.66	33.16	91.74	91.57
	Mean(SD)	**117.54(73.72)**	**153.18(55.53)**	**38.26(17.62)**	**62.83(21.82)**	**77.90(36.16)**	**108.00(24.29)**
Additive VcVS	1	58.54	137.28	28.41	66.79	43.48	102.04
	2	20.83	60.30	49.68	104.49	35.26	82.40
	3	177.09	248.66	35.20	64.19	106.14	156.43
	4	131.68	109.51	42.67	59.90	87.18	84.71
	5	127.16	143.04	26.88	34.82	77.02	88.93
	Mean(SD)	**103.06(62.5)**	**139.76(69.11)**	**36.57(9.64)**	**66.04(24.97)**	**69.82(29.84)**	**102.90(30.87)**
No Stim Control	1	48.79	73.09	42.75	54.54	45.77	63.82
	2	54.16	58.92	111.21	104.04	82.68	81.48
	3	233.73	196.97	72.64	72.14	153.18	134.55
	4	152.14	71.22	82.56	72.22	117.35	71.72
	5	142.23	144.60	38.92	34.33	90.58	89.47
	Mean(SD)	**126.21(76.93)**	**108.96(59.65)**	**69.61(29.88)**	**67.45(25.73)**	**97.91(40.12)**	**88.21(27.67)**
Non Correlated Control	1	79.38	35.92	29.83	16.40	54.61	26.16
	2	55.09	67.70	67.98	51.24	61.54	59.47
	3	115.59	73.56	29.19	22.42	72.39	47.99
	4	158.09	143.84	44.39	41.82	101.24	92.83
	5	163.14	137.35	25.28	15.60	94.21	76.48
	Mean(SD)	**114.26(47.51)**	**91.67(46.95)**	**39.33(17.58)**	**29.50(16.12)**	**76.80(20.28)**	**60.59(25.68)**

Figure 17 Pooled subject data - Exp 2 Muscular response - magnitude of medium latency response in TFL, MG and combined EMG (non normalized)

Magnitude of the medium latency responses (non normalized for background EMG) of TFL, MG and combined EMG recordings from all subjects (n=5), (Fischer's LSD, $P < 0.005$; significance denoted by (*)).

RMS values of EMG (mV)

Trial	Subject	TFL(10^2)		MG	
		Pre	**Post**	**Pre**	**Post**
Subtractive VcVS	1	2.42	2.07	0.10	0.09
	2	2.48	2.19	0.22	0.18
	3	4.49	3.61	0.09	0.08
	4	3.49	3.17	0.08	0.08
	5	3.95	2.47	0.05	0.04
	Mean(SD)	**3.36(0.91)**	**2.70(0.67)**	**0.11(0.06)**	**0.09(0.05)**
Additive VcVS	1	2.24	2.02	0.09	0.08
	2	2.12	1.75	0.22	0.16
	3	4.00	3.26	0.09	0.08
	4	4.03	2.75	0.09	0.08
	5	2.22	1.96	0.04	0.04
	Mean(SD)	**2.92(1.00)**	**2.35(0.63)**	**0.11(0.07)**	**0.09(0.04)**
No Stim Control	1	1.36	1.44	0.07	0.07
	2	1.28	1.51	0.17	0.17
	3	2.55	2.12	0.09	0.08
	4	2.32	1.17	0.08	0.07
	5	2.02	2.14	0.04	0.04
	Mean(SD)	**1.91(0.57)**	**1.68(0.43)**	**0.09(0.05)**	**0.09(0.04)**
Non Correlated Control	1	2.35	2.35	0.08	0.09
	2	2.36	2.47	0.20	0.21
	3	3.28	2.99	0.08	0.07
	4	4.74	3.96	0.10	0.08
	5	3.15	3.15	0.04	0.04
	Mean(SD)	**3.18(0.98)**	**2.98(0.64)**	**0.10(0.06)**	**0.10(0.07)**
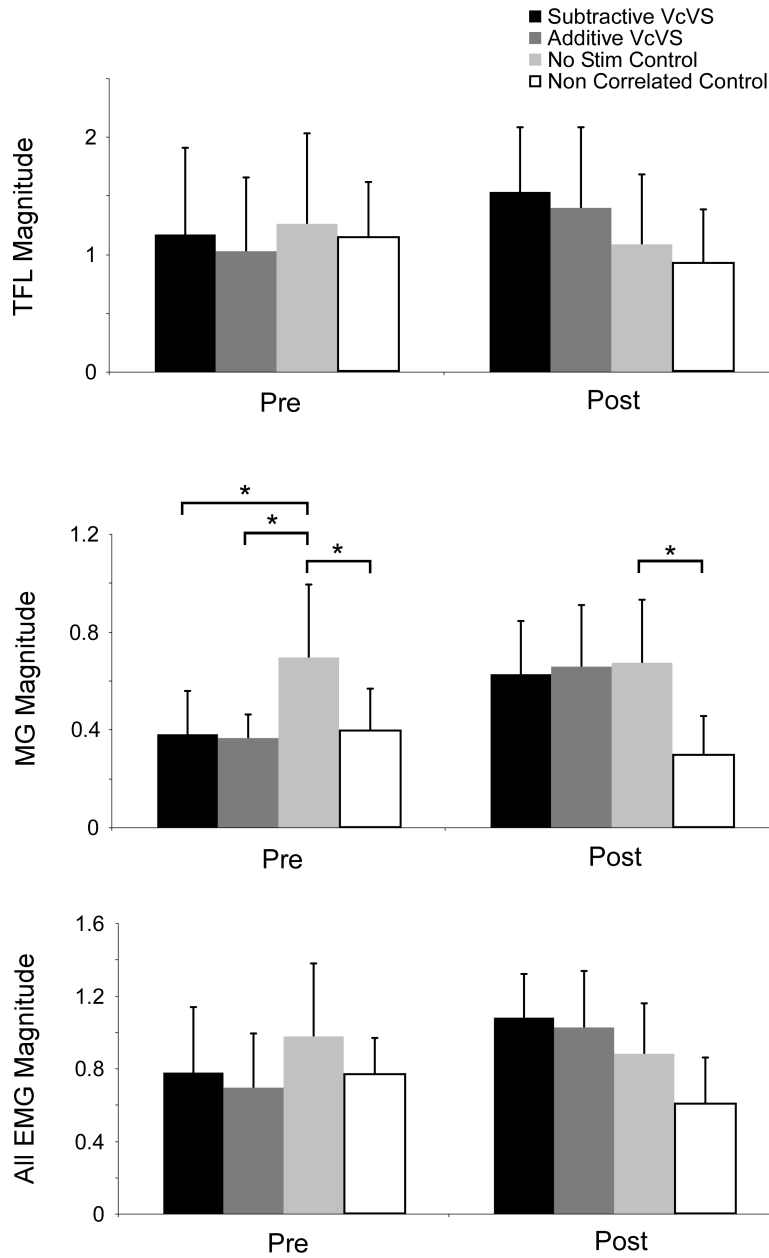
Figure 18 Pooled subject data - Exp 2 Muscular response - RMS values of EMG recording in TFL and MG
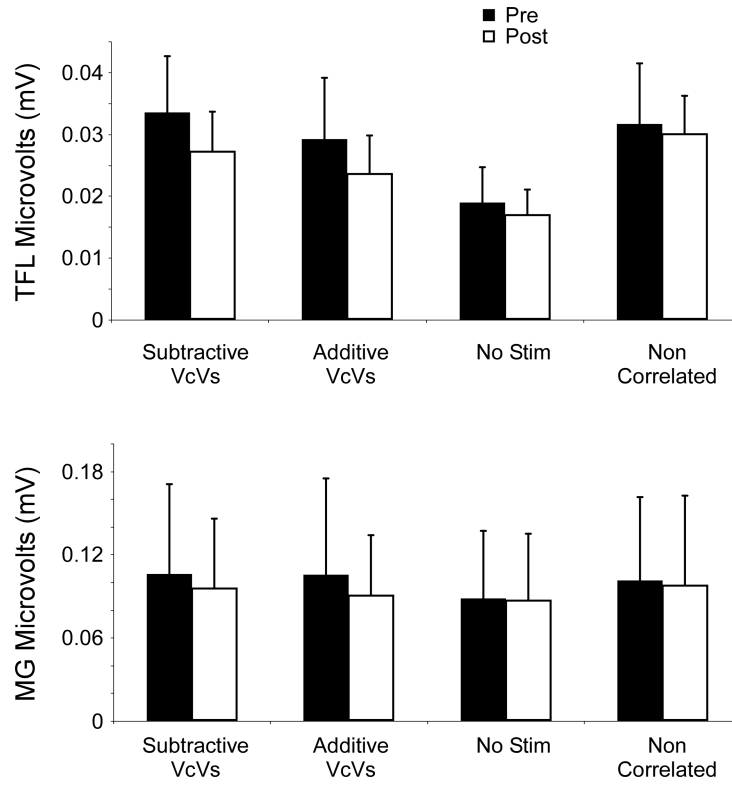
Figure 19 Pooled subject data - Exp 2 Muscular response - coherence
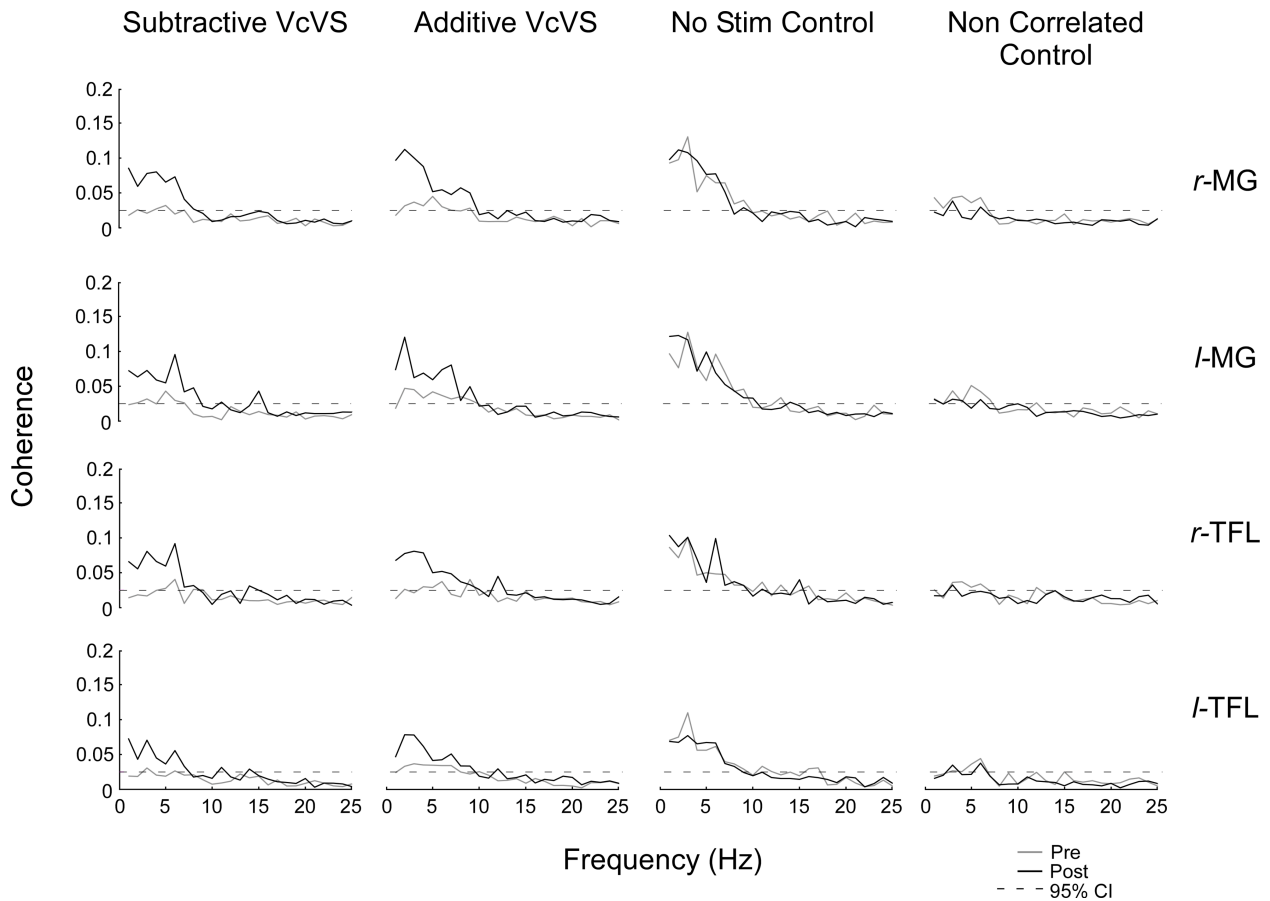
Coherence analyses for pooled subject data were completed for each subject using segments of 2^{11} data points in order to determine the amount of linear correlation in the frequency domain between the SVS and EMG signals. Data from two trials of the same stimulus type were concatenated to produce 120 windows generating a frequency resolution of 1 Hz (1 s/segment). Gain and phase analyses for pooled subject data were completed using 2^{13} data points and produced 30 windows generating a frequency resolution of 0.25 Hz (4 s/segment).

*Figure 20 Pooled subject data - Exp 2 Muscular response - gain and phase*
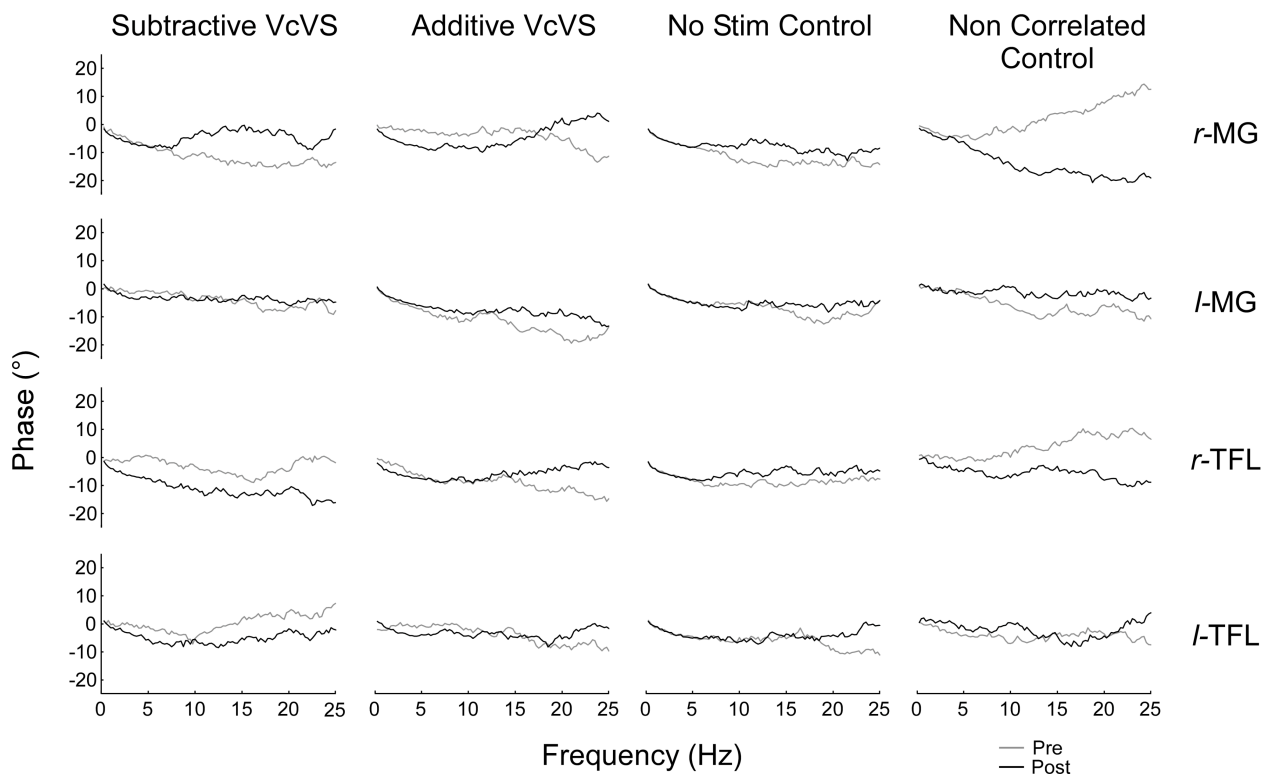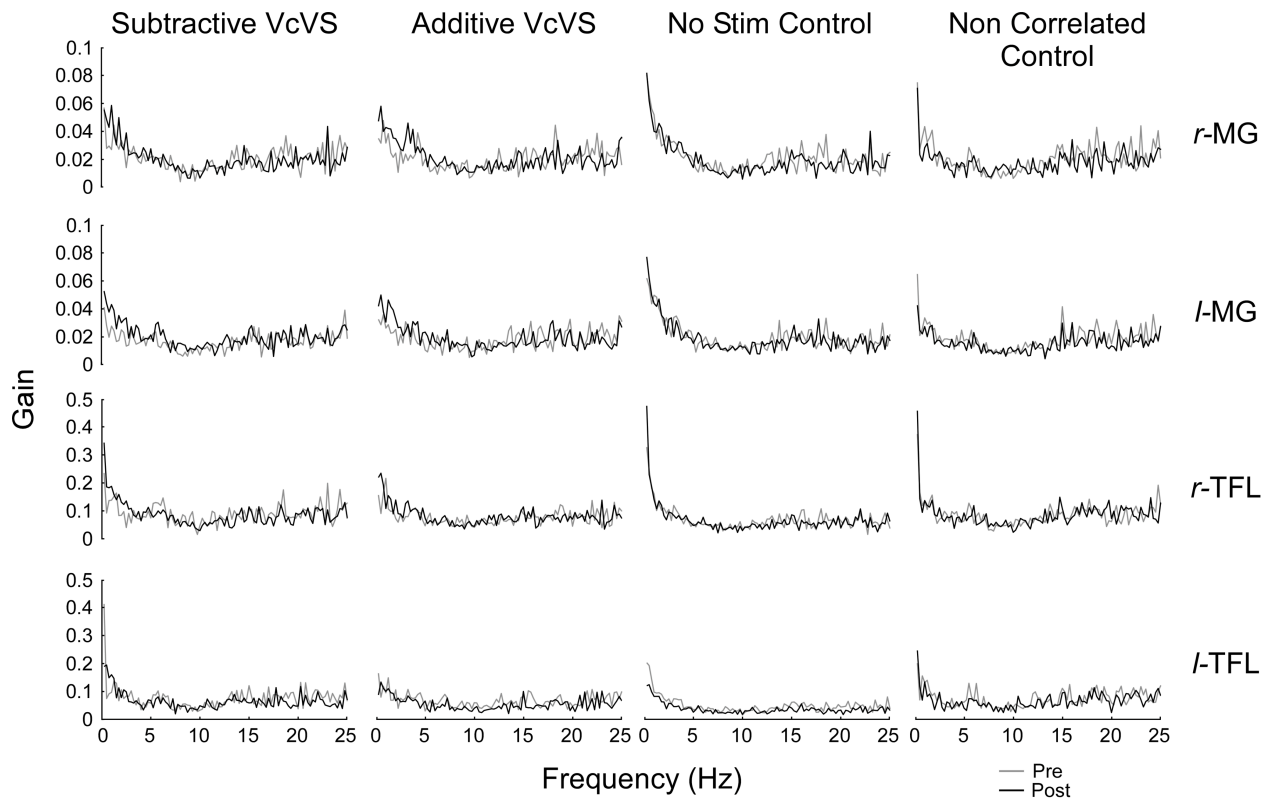
Table 13 Subject data - Comparison of normalized and non normalized data

Peak amplitude of medium latency response

	Subject	Non normalized		Normalized	
MG(10^2)		EC	EO	EC	EO
	1	0.56	0.23	13.58	8.50
	2	0.41	0.25	9.72	10.40
	3	0.47	0.19	10.11	6.90
	4	0.32	0.17	10.98	9.96
	5	0.21	0.17	6.44	7.60
	6	0.49	0.11	12.25	6.26
	Mean(SD)	**0.41(0.13)**	**0.19(0.05)**	**10.51(2.45)**	**8.27(1.66)**
TFL(10^2)		EC	EO	EC	EO
	1	1.63	0.30	12.97	5.32
	2	0.86	0.37	5.39	3.93
	3	1.85	0.40	7.05	4.15
	4	1.03	0.19	8.53	5.87
	5	0.86	0.24	9.34	7.43
	6	0.91	0.14	7.74	3.19
	Mean(SD)	**1.19(0.44)**	**0.27(0.10)**	**8.50(2.57)**	**4.98(1.54)**

Pilot study: Subjects (n=6) stood on foam and received 2 mA peak to peak (0-25 Hz) SVS signal for 60 s. Muscle activity was recorded bilaterally from MG and TFL. Two trials were with eyes closed and two trials were with eyes open. Two alike trials were concatenated to give 120 s of data. Cumulant density estimates were used to represent the time-domain relationship between SVS and muscle activity (non normalized). For the normalized results, the cumulant density estimates were divided by the product of the vector norms of the SVS and EMG signals. The peak amplitude of the medium latency response was extracted and compared.

Figure 21 Pooled subject data - Peak amplitude of normalized and non normalized data from MG and TFL
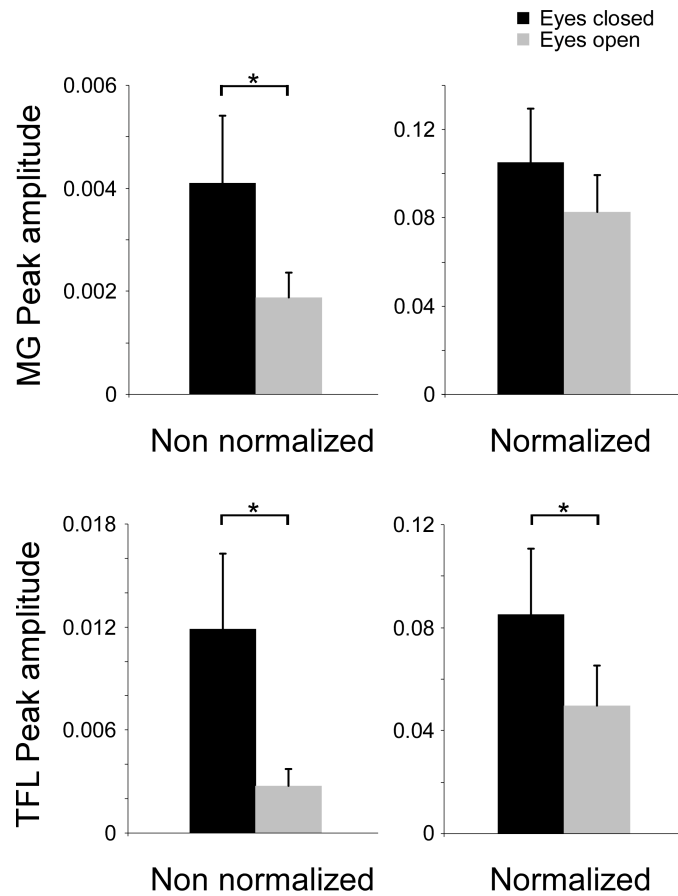
Peak amplitude of the medium latency responses of MG and TFL recordings from all subjects (n=6), (Dependent samples T-test, P < 0.05; significance denoted by (*)).